Jet Propulsion Laboratory
California Institute of Technology

Evolution of the TOPEX products from MGDR-B to GDR-F over 1992-2002

Jet Propulsion Laboratory, California Institute of Technology
Matthieu Talpe on behalf of the JPL Cal/Val team

Virtual OSTST 2020, October 19-23

The updates in the TOPEX products since their last release (MGDR-B) cover all components.

Components	MGDR-B	GDR-F
Altimeter parameters	Onboard	Numerical Retracking
Range correction	Wallops Cal1	Numerical Retracking
Sigma0 correction	Wallops Climatological	Numerical Retracking
Radiometer Sigma0 attenuation	Uncalibrated	Calibrated
Radiometer wet path delay	Uncalibrated	Calibrated + coastal retrieval
Dry tropospheric correction	ECMWF Operational (no S1/S2)	ERA Interim + S1/S2
Model wet path delay	ECMWF Operational	ERA Interim
Sea State Bias	Parametric (Gaspar et al., 1994)	Non-Parametric (Putnam et al., 2020), TBC
Wind speed	Witter and Chelton (1995)	Collard (2005)
Orbits	Operational: GSFC and CNES	Reprocessed ITRF14: GSFC and CNES
Geophysical corrections	1990s standards	GDR-F

How does each component update influence the final sea surface height anomaly (SSHA)?

In answering this question, this presentation examines three metrics:

1. **The SSHA curve**
2. **Timeseries of SSHA crossover RMS**
3. **Maps of SSHA crossover means**

For each metric, we first start with the original MGDR-B SSHA version, then subsequently replace targeted MGDR-B components with their GDR-F equivalent, and ultimately recover the full GDR-F SSHA.

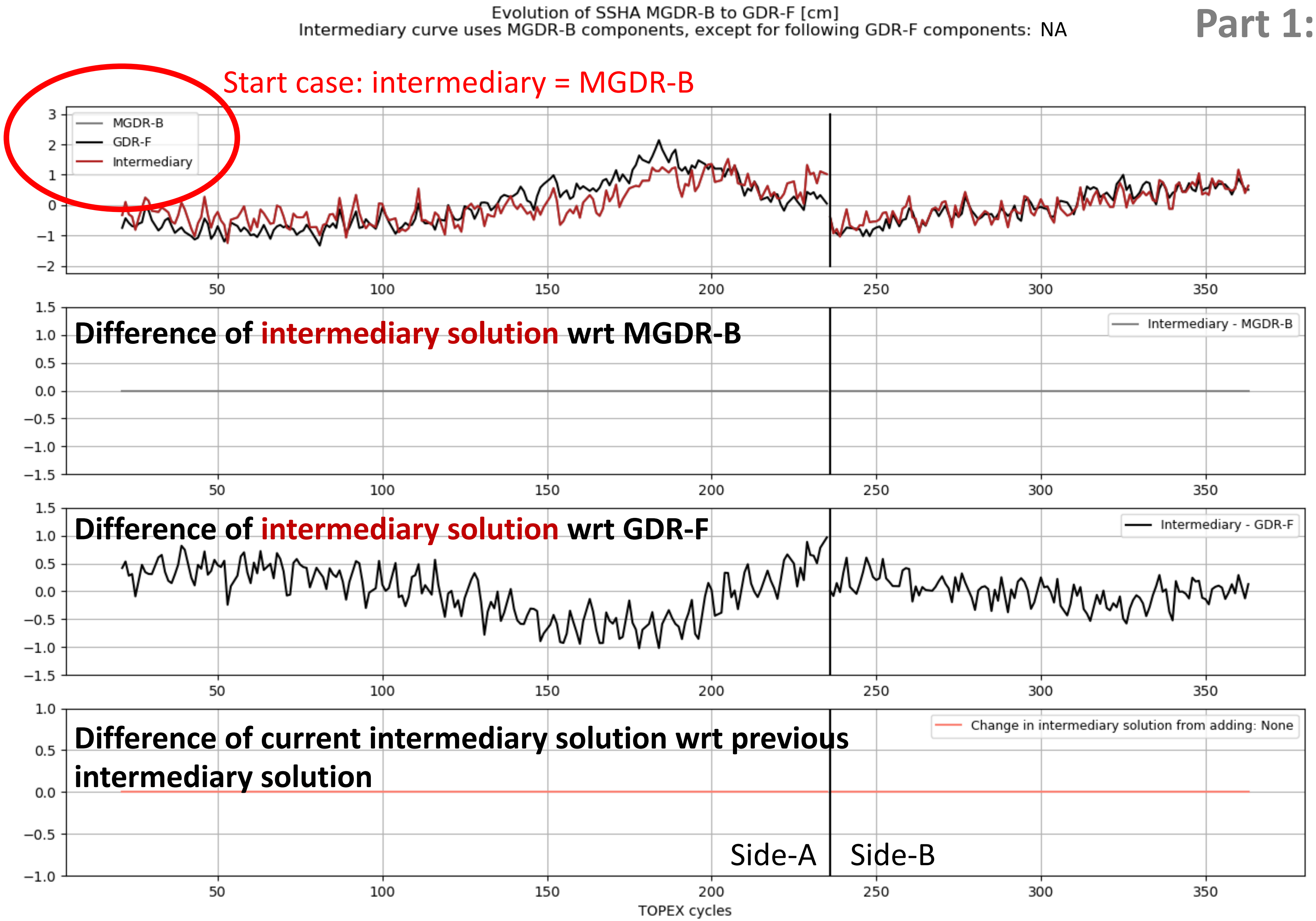

Notes: **1)** MGDR-B already has IB correction from GDR-F **2)** Seasonality + bias have been removed, i.e., **side-A vs side-B bias is not visible.**

Adding GDR-F: **Geophysical models (pole, solid earth, ocean tides, and MSS)**

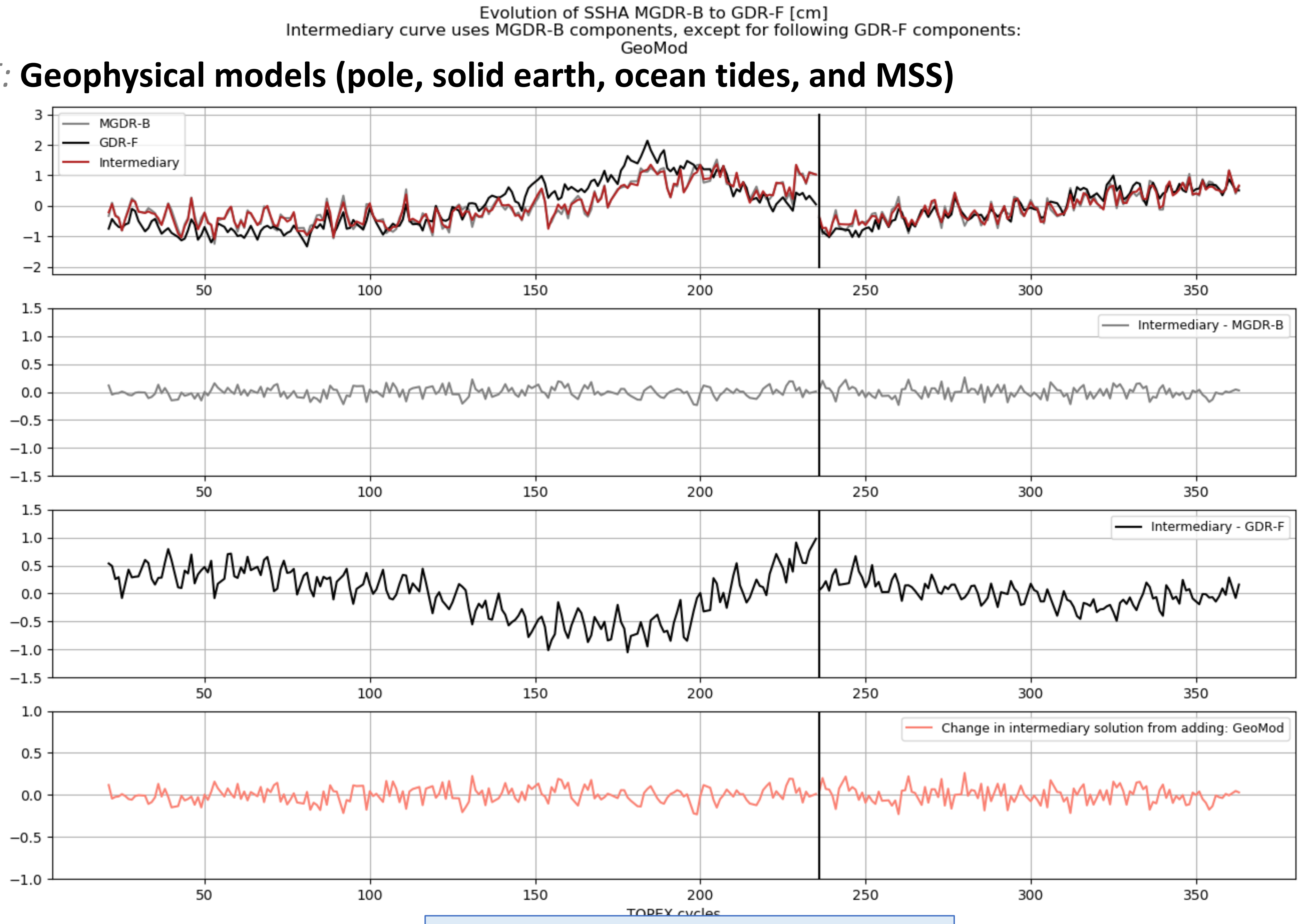

→ Induces ~3 mm level differences

Adding GDR-F: **Orbit (GSFC)**

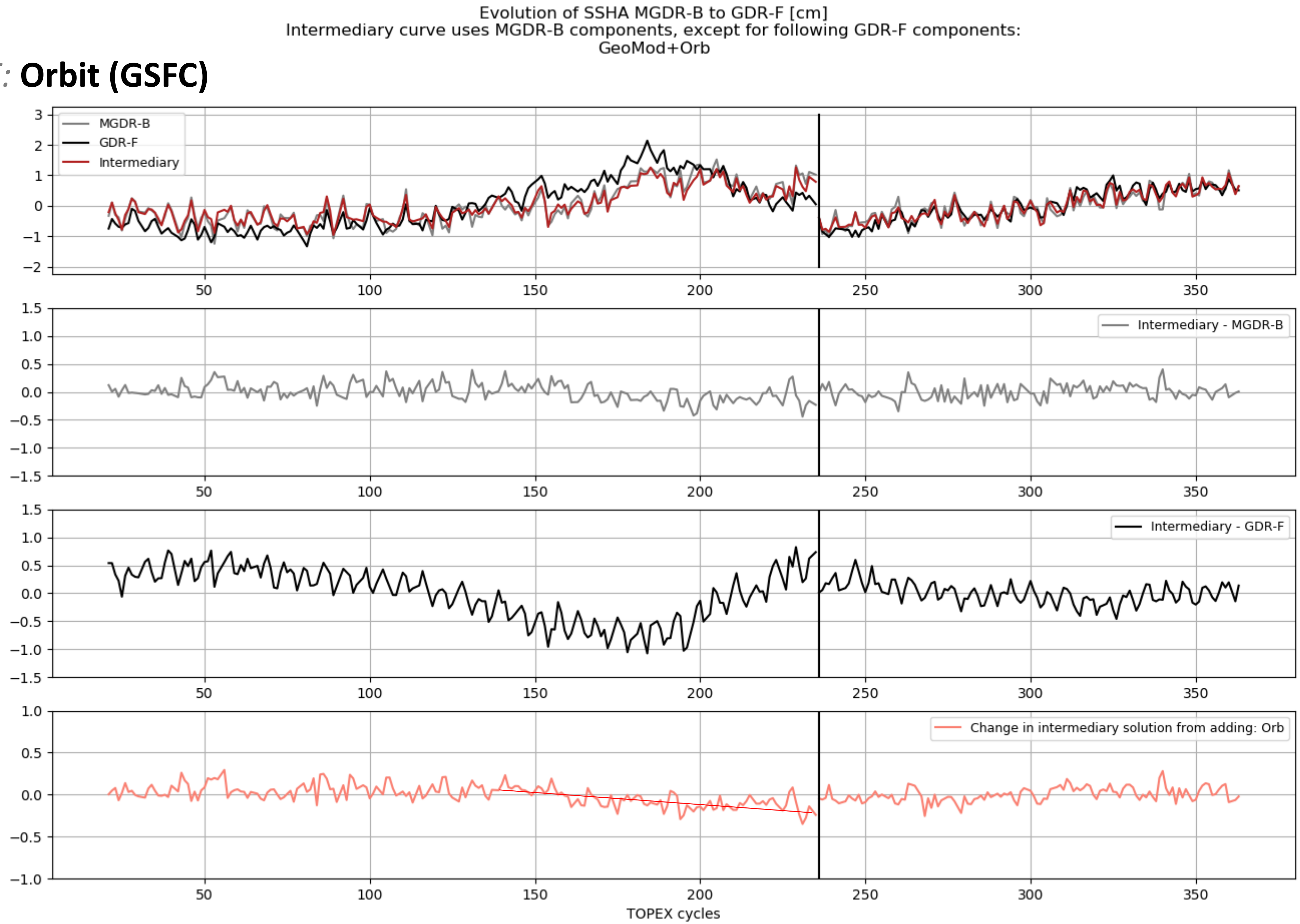

→ ~3 mm drop over the last 90 cycles of side-A

Adding GDR-F: **Dry tropo**

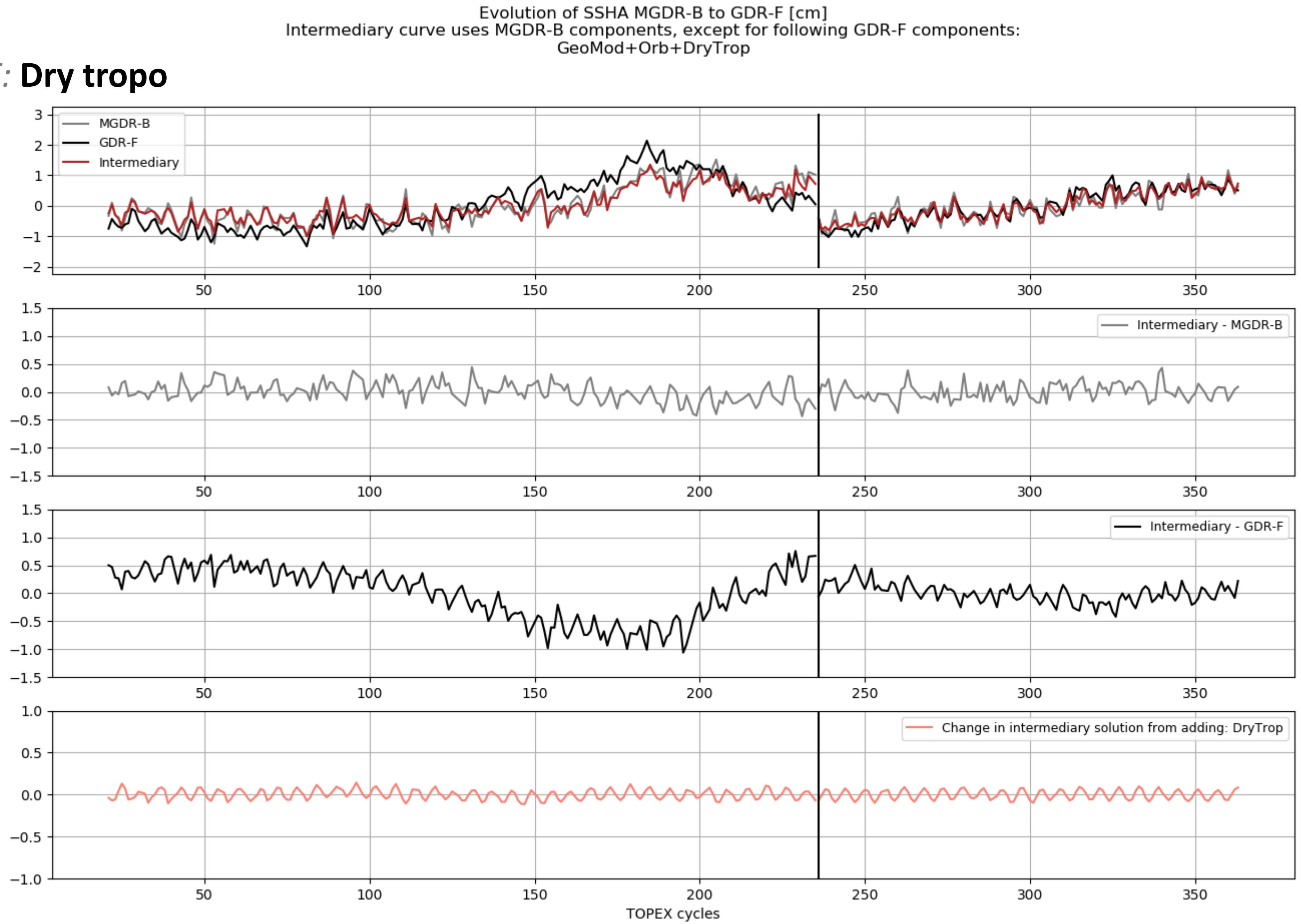

→ Removes mm-level 60-day signal that was due to omission of S1/S2 atmospheric tides in MGDR-B dry tropo model

Adding GDR-F: **Radiometer wet path delay**

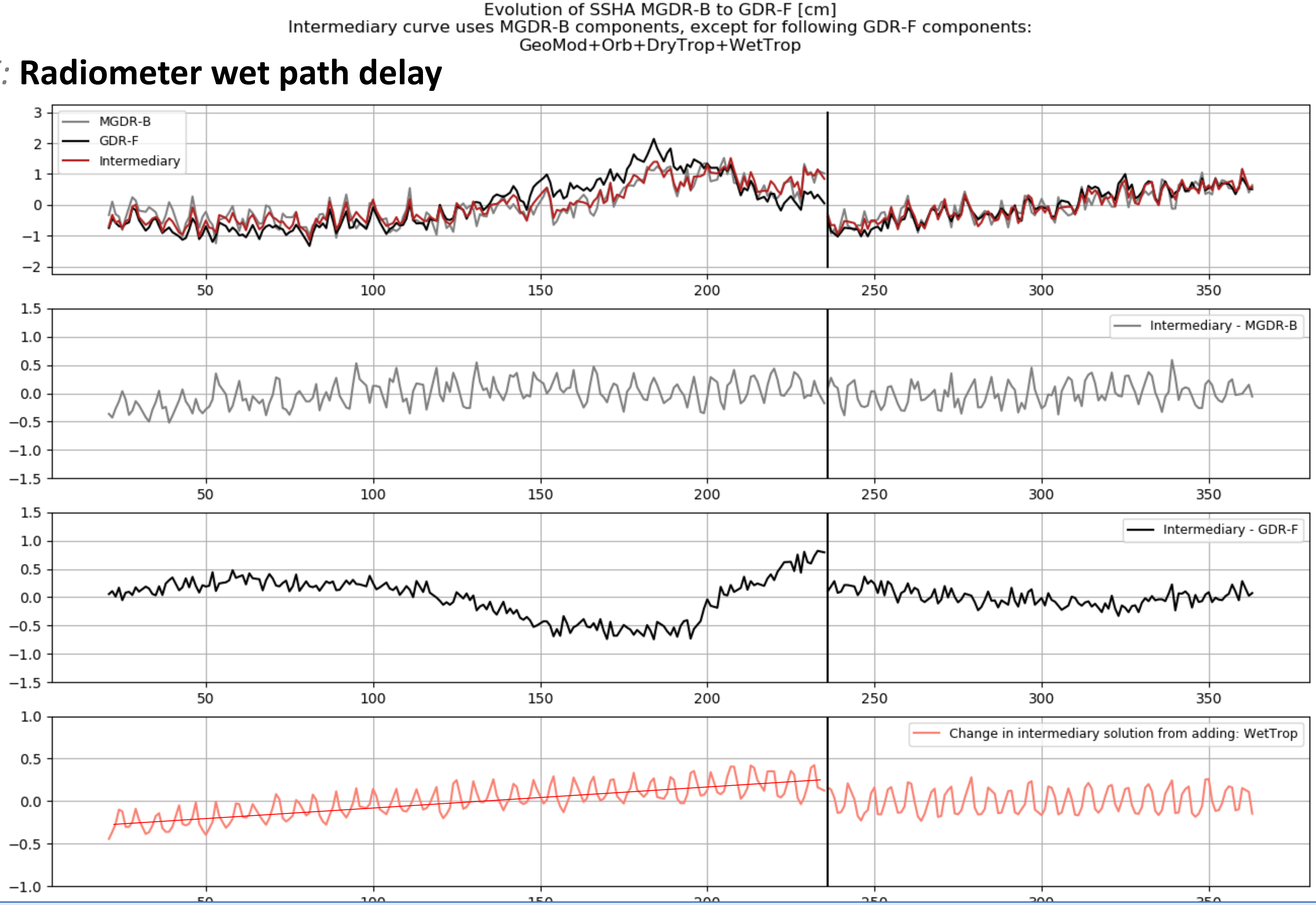

→ End-of-mission recalibration of radiometer mitigates 1) ~4mm 60-day signal caused by yaw-state dependent thermal environment, 2) -0.9 mm/yr drift over side A.

Adding GDR-F: **Sea state bias (Putnam et al., OSTST 2020)**

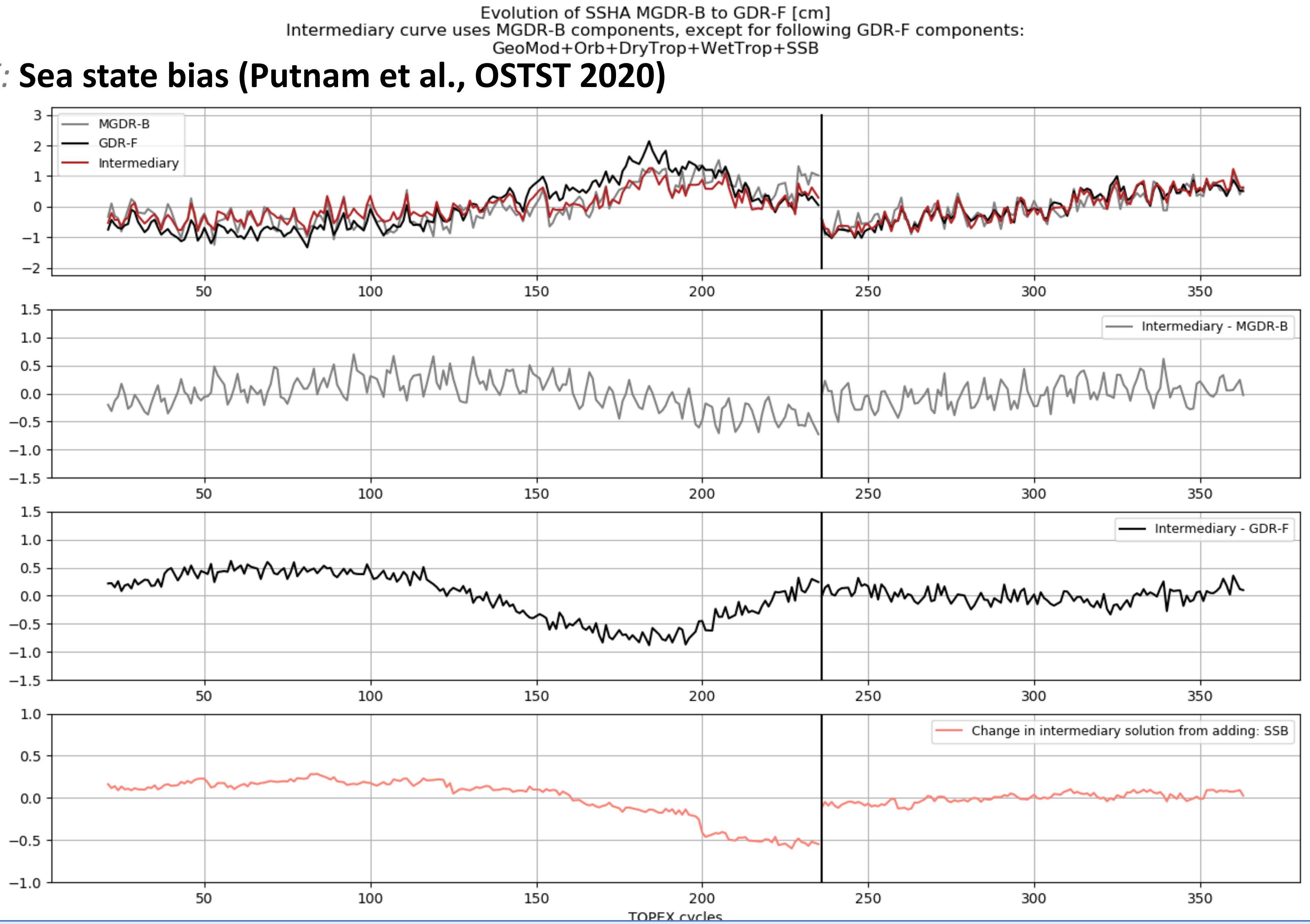

→ Waveform retracking mitigates SWH degradation, especially at end of side A, and reduces drift from sea state bias

Adding GDR-F: **Ionospheric correction**

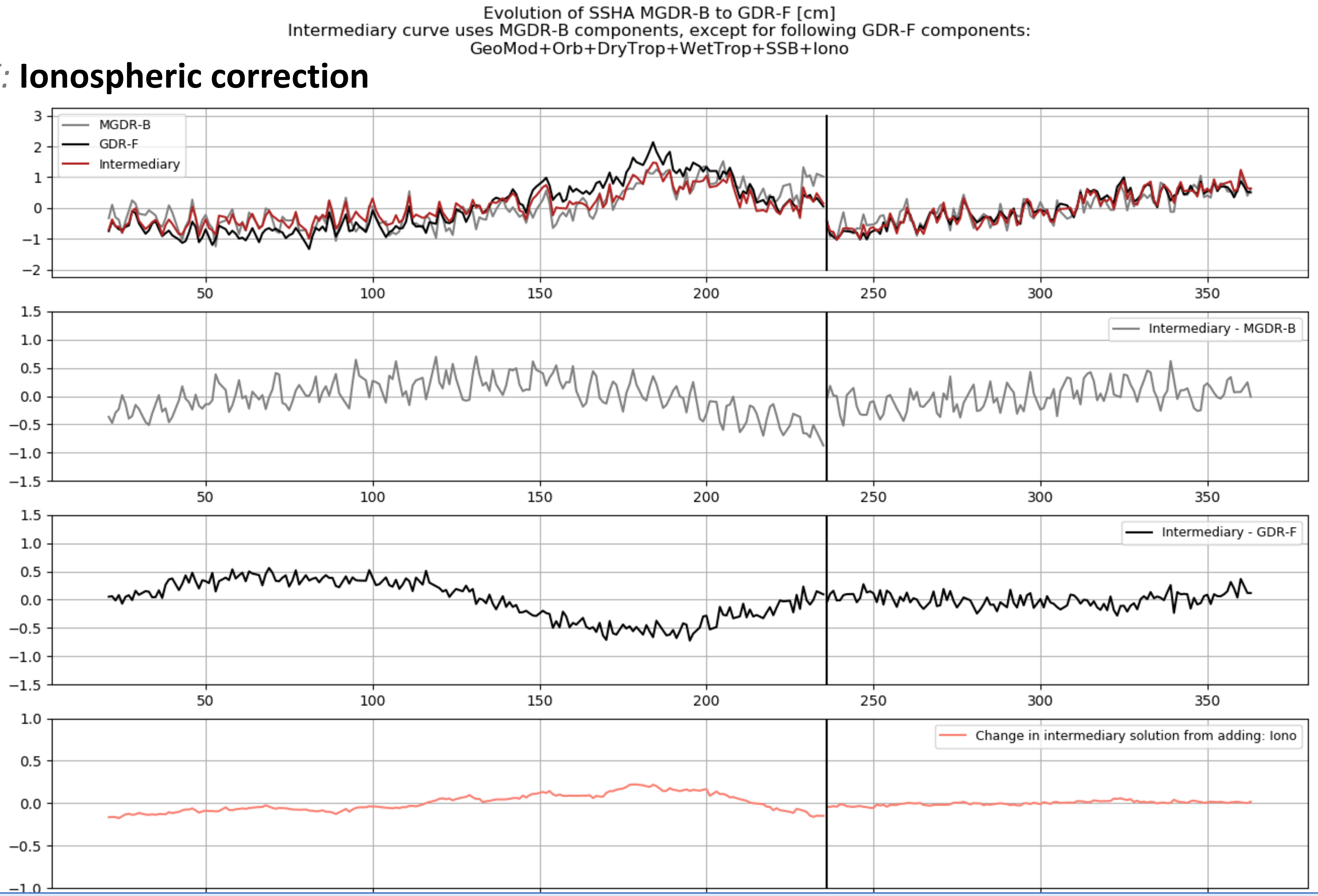

→ Ku- and C-band waveform retracking reduces +/- 3 mm temporal variation in ionosphere correction, primarily during side A.

Adding GDR-F: **Numerically retracked range (Desjonquères et al., OSTST 2019)**

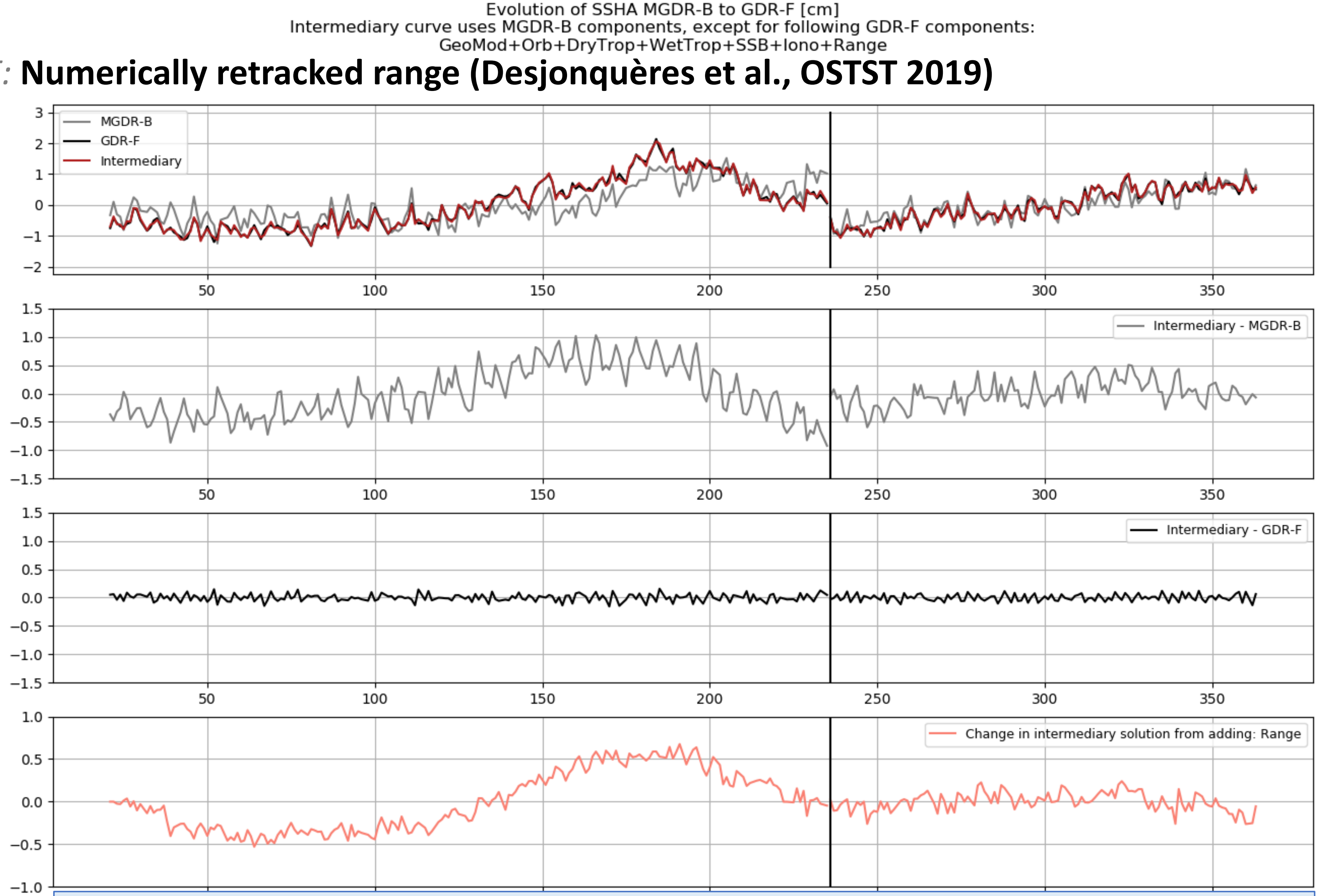

→ Waveform retracking results with +/- 5 mm variations in range. Note: the MGDR-B range includes onboard Wallops correction.

Adding GDR-F: **internal tide, high-frequency fluctuations, non-equil. ocean tide (new additions in GDR-F standard)**

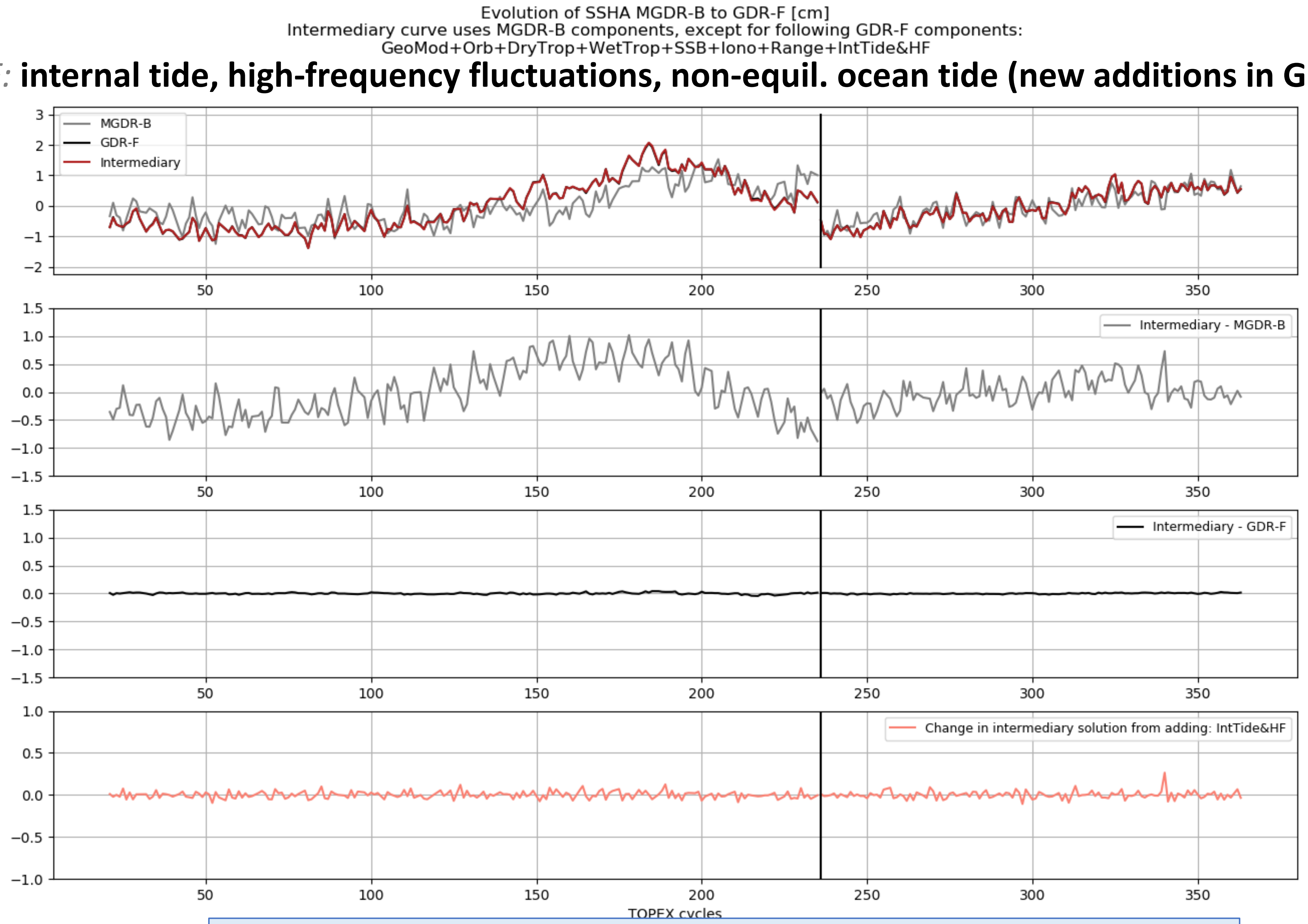

→ Reduces noise to sub-mm (remaining noise due to updates in flags)

How does each component update influence the final sea surface height anomaly (SSHA)?

1. **The SSHA curve**
   - ➢ The updates over side-B are stable in time and stochastic in nature, aside from the atmospheric path delays.
   - ➢ In contrast, side-A contains notable systematic differences between MGDR-B and GDR-F. The dominant difference stems from the numerically retracked ranges and reprocessed calibrations, which induce a cm-level, evolving signal (see Desjonquères et al., OSTST 2019). Accordingly, the ionosphere and SSB corrections also contribute several mms to SSHA differences at the end of side-A.
   - ➢ The update in geophysical models modifies the SSHA curve by a stochastic signal with an amplitude of ~3 mm.
   - ➢ The reprocessed radiometer data corroborate a near-mm/yr drift difference in the wet path delay over side-A.
   - ➢ The updated orbit also shows a 3-mm drop over the last 2.5 years of side-A.
   - ➢ The new wet and dry tropospheric path delays entail changes of mm-level, 60-day periodic signals.
2. **Timeseries of SSHA crossover RMS**
3. **Maps of SSHA crossover means**

How does each component update influence the final sea surface height anomaly (SSHA)?

1. **The SSHA curve**
   - The updates over side-B are stable in time and stochastic in nature, aside from the atmospheric path delays.
   - In contrast, side-A contains notable systematic differences between MGDR-B and GDR-F. The dominant difference stems from the numerically retracked ranges and reprocessed calibrations, which induce a cm-level, evolving signal (see Desjonquères et al., OSTST 2019). Accordingly, the ionosphere and SSB corrections also contribute several mms to SSHA differences at the end of side-A.
   - The update in geophysical models modifies the SSHA curve by a stochastic signal with an amplitude of ~3 mm.
   - The reprocessed radiometer data corroborate a near-mm/yr drift difference in the wet path delay over side-A.
   - The updated orbit also shows a 3-mm drop over the last 2.5 years of side-A.
   - The new wet and dry tropospheric path delays entail changes of mm-level, 60-day periodic signals.
2. **Timeseries of SSHA crossover RMS**
3. **Maps of SSHA crossover means**

The overall measurement performance remains stable over the two TOPEX sides.

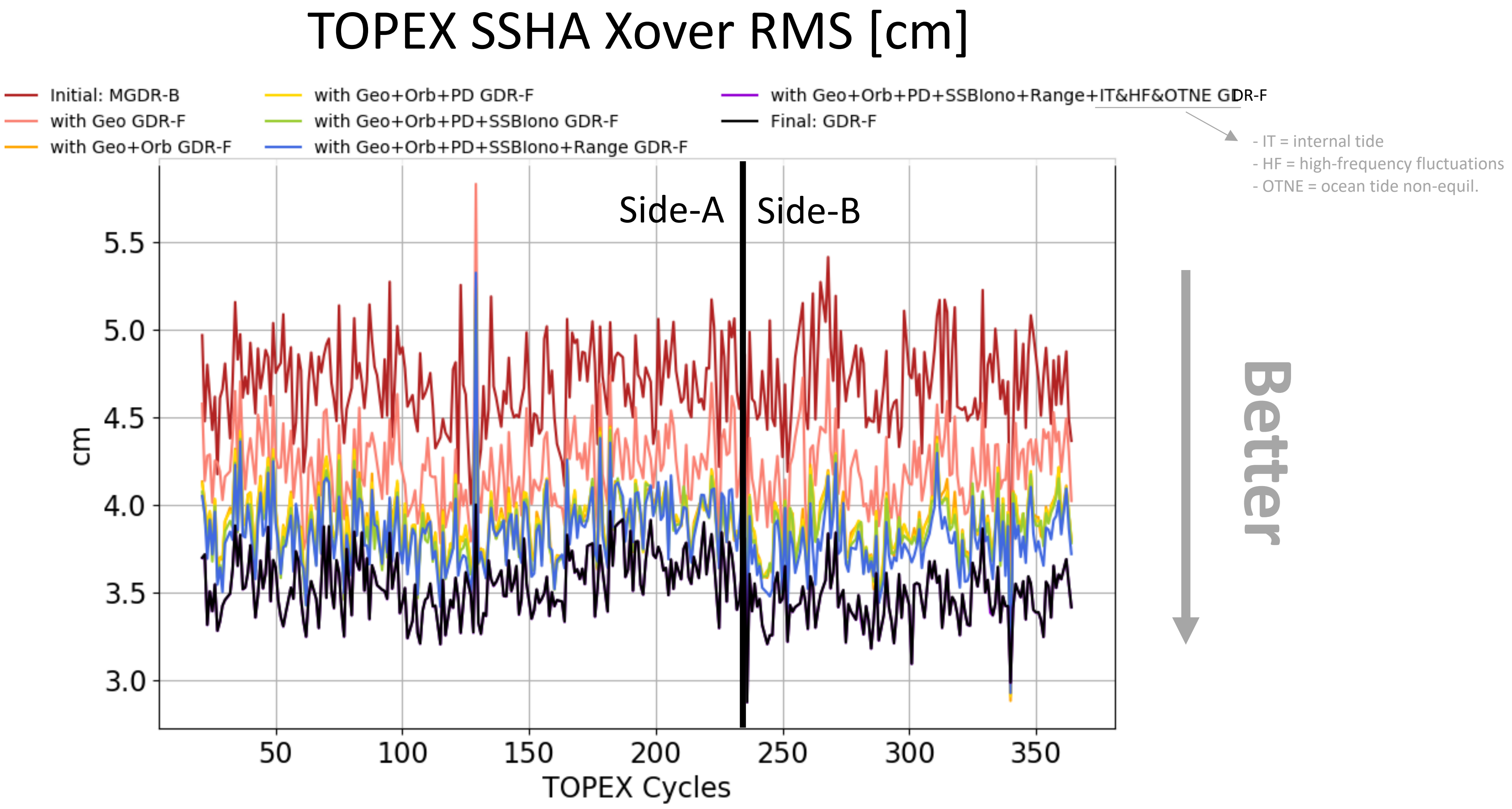

Note: The crossover points are selected based on editing criteria that include latitude range of [-45; 45] degree, inverse barometric correction range of [-0.15; 0.15] m, altimeter wind speed range of [4; 10] m/s, and SWH range of [1; 4] m.

The total variance reduction for SSHA crossovers between MGDR-B and GDR-F is nearly 1000 mm².

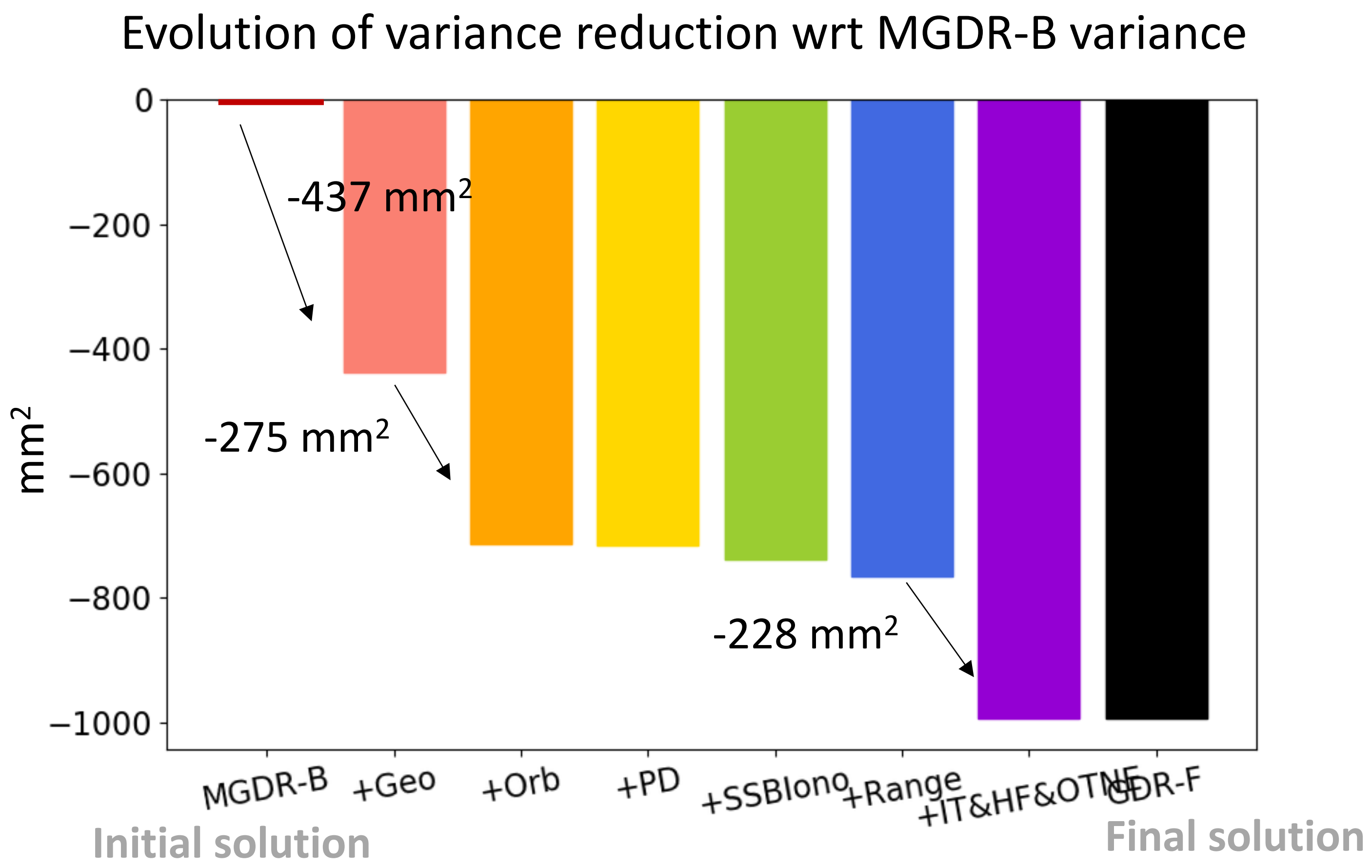

- Using the GDR-F geophysical models leads to a variance reduction of 437 mm^2 – the largest reduction observed. Using the GDR-F orbits also leads to a large variance reduction of 275 mm^2.
- Adding internal-tide, ocean tide non-equil, and high-frequency fluctuations together reduce variance by 228 mm^2. The high-frequency fluctuations component is the main contributor.

How does each component update influence the final sea surface height anomaly (SSHA)?

1. **The SSHA curve**
   - The updates over side-B are stable in time and stochastic in nature, aside from the atmospheric path delays.
   - In contrast, side-A contains notable systematic differences between MGDR-B and GDR-F. The dominant difference stems from the numerically retracked ranges and reprocessed calibrations, which induce a cm-level, evolving signal (see Desjonquères et al., OSTST 2019). Accordingly, the ionosphere and SSB corrections also contribute several mms to SSHA differences at the end of side-A.
   - The update in geophysical models modifies the SSHA curve by a stochastic signal with an amplitude of ~3 mm.
   - The reprocessed radiometer data corroborate a near-mm/yr drift difference in the wet path delay over side-A.
   - The updated orbit also shows a 3-mm drop over the last 2.5 years of side-A.
   - The new wet and dry tropospheric path delays entail changes of mm-level, 60-day periodic signals.
2. **Timeseries of SSHA crossover RMS**
   - The dominant contributors to lowering variance from MGDR-B to GDR-F are the geophysical models, orbits, and high-frequency fluctuations; SSHA crossover variance is reduced by 437, 275, and 228 mm^2, respectively.
   - In contrast, the wet and dry tropospheric path delays contribute minimally.
3. **Maps of SSHA crossover means**

How does each component update influence the final sea surface height anomaly (SSHA)?

1. **The SSHA curve**
   - The updates over side-B are stable in time and stochastic in nature, aside from the atmospheric path delays.
   - In contrast, side-A contains notable systematic differences between MGDR-B and GDR-F. The dominant difference stems from the numerically retracked ranges and reprocessed calibrations, which induce a cm-level, evolving signal (see Desjonquères et al., OSTST 2019). Accordingly, the ionosphere and SSB corrections also contribute several mms to SSHA differences at the end of side-A.
   - The update in geophysical models modifies the SSHA curve by a stochastic signal with an amplitude of ~3 mm.
   - The reprocessed radiometer data corroborate a near-mm/yr drift difference in the wet path delay over side-A.
   - The updated orbit also shows a 3-mm drop over the last 2.5 years of side-A.
   - The new wet and dry tropospheric path delays entail changes of mm-level, 60-day periodic signals.
2. **Timeseries of SSHA crossover RMS**
   - The dominant contributors to lowering variance from MGDR-B to GDR-F are the geophysical models, orbits, and high-frequency fluctuations; SSHA crossover variance is reduced by 437, 275, and 228 mm^2, respectively.
   - In contrast, the wet and dry tropospheric path delays contribute minimally.
3. **Maps of SSHA crossover means**

The maps of mean SSHA crossovers show smaller geographically-correlated errors in GDR-F.

Side-A

Xover mean of MGDR-B [cm]

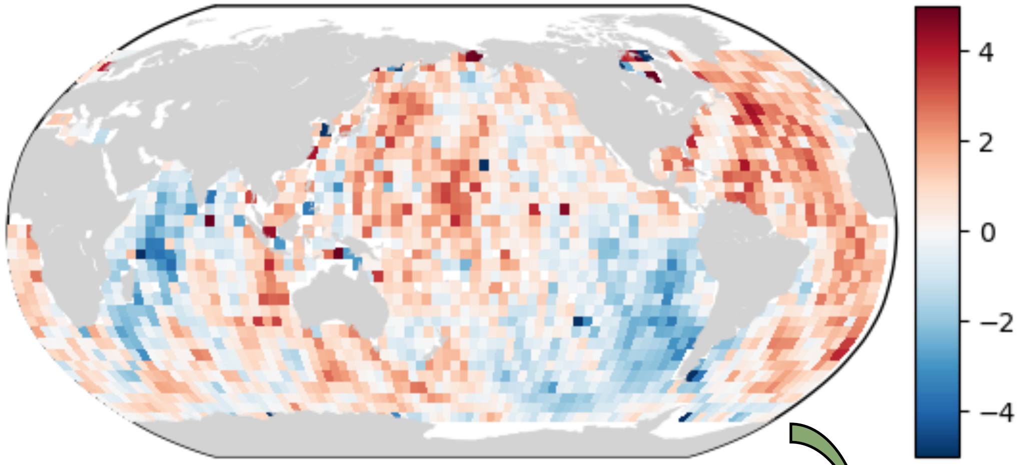

Xover mean of GDR-F [cm]

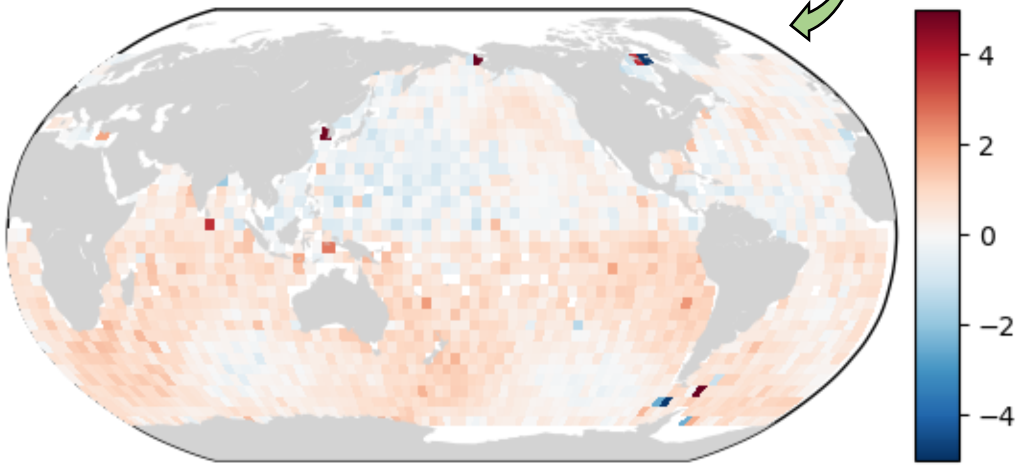

Starting solution is MGDR-B

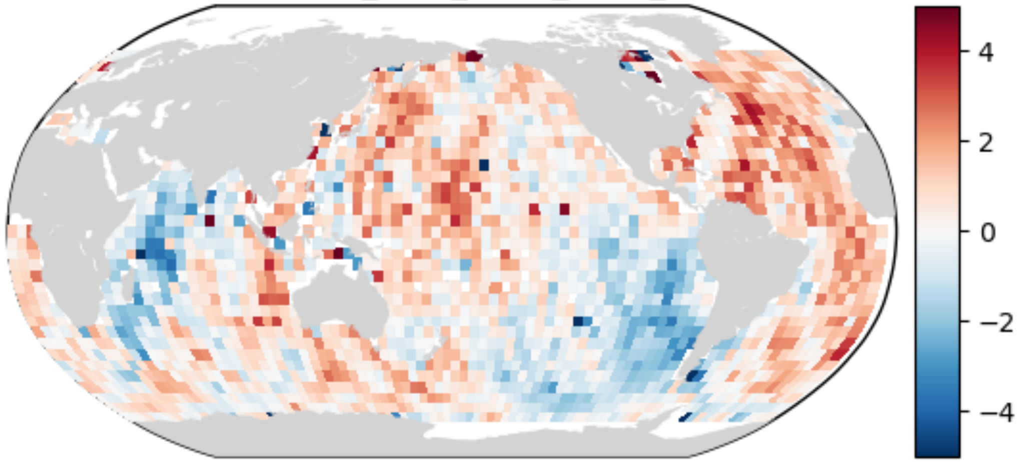

Difference wrt Xover mean MGDR-B [cm]

Xover mean wrt previous solution [cm]

NA

Difference wrt Xover mean GDR-F [cm]

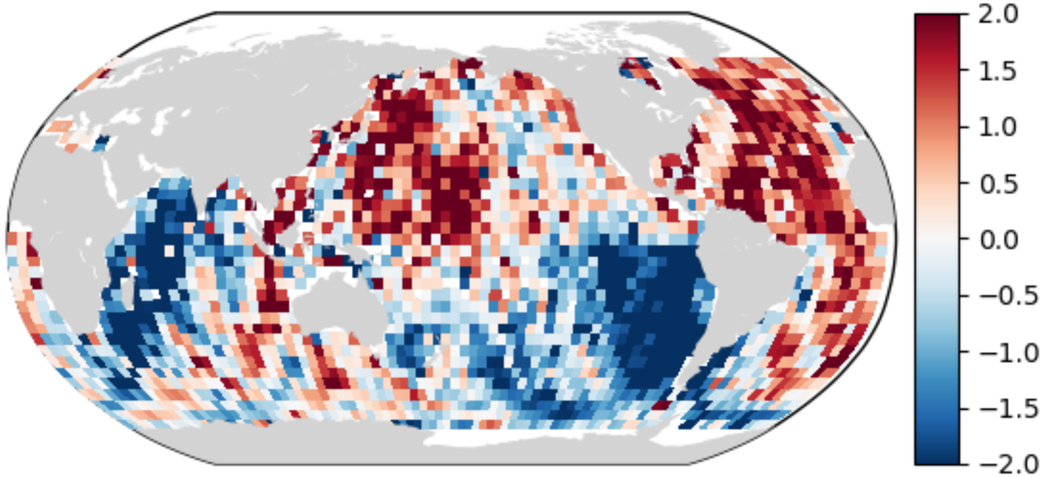

Adding GDR-F: **Geophysical models (pole, solid earth, ocean tides and MSS)**

Xover mean of intermediary SSHA solution [cm]

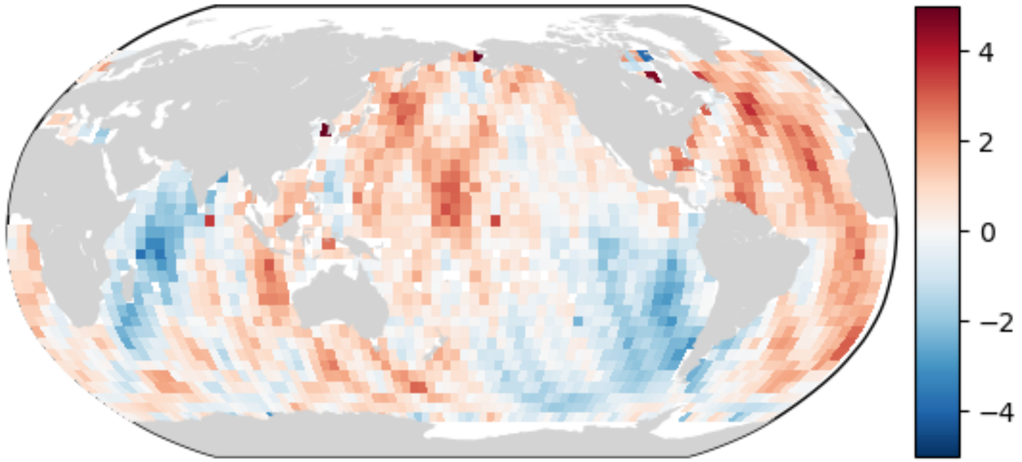

Difference wrt Xover mean MGDR-B [cm]

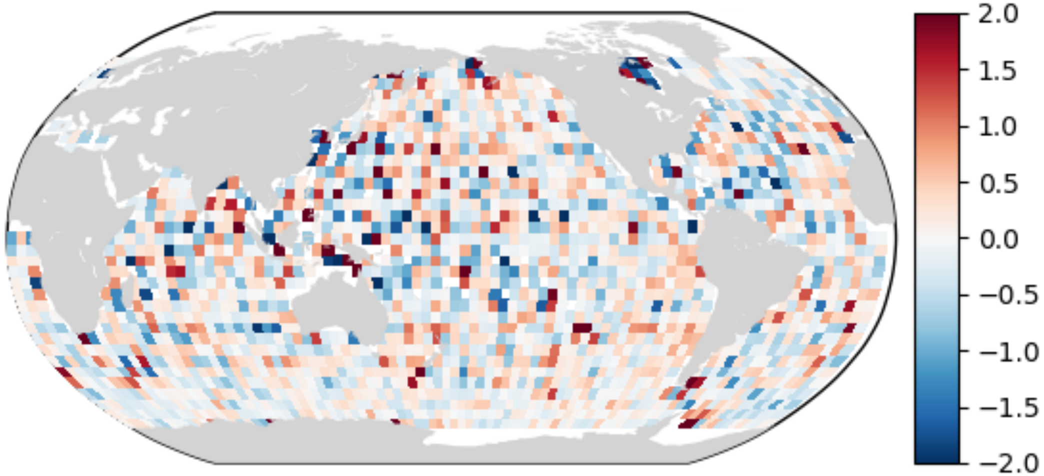

Difference wrt previous solution [cm]

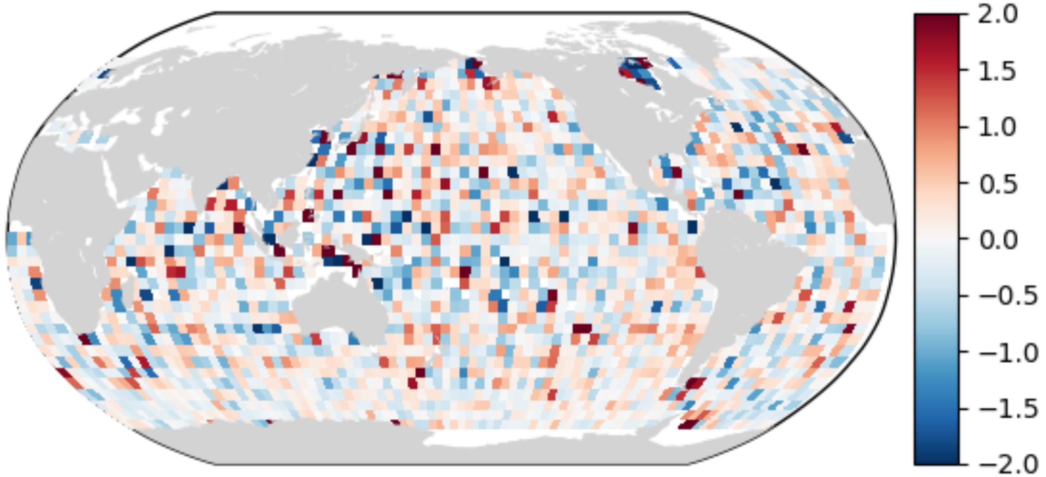

Difference wrt Xover mean GDR-F [cm]

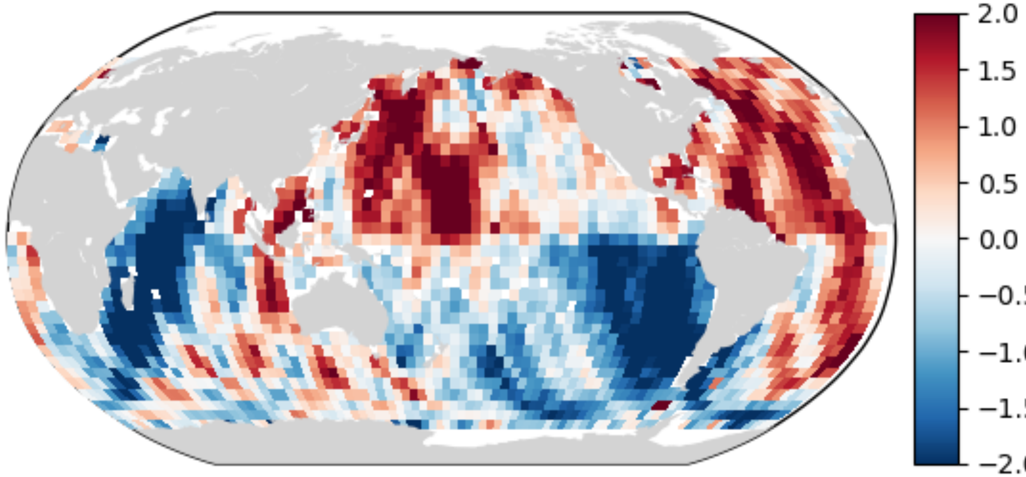

Adding GDR-F: **Orbit (GSFC)**

Xover mean of intermediary SSHA solution [cm]

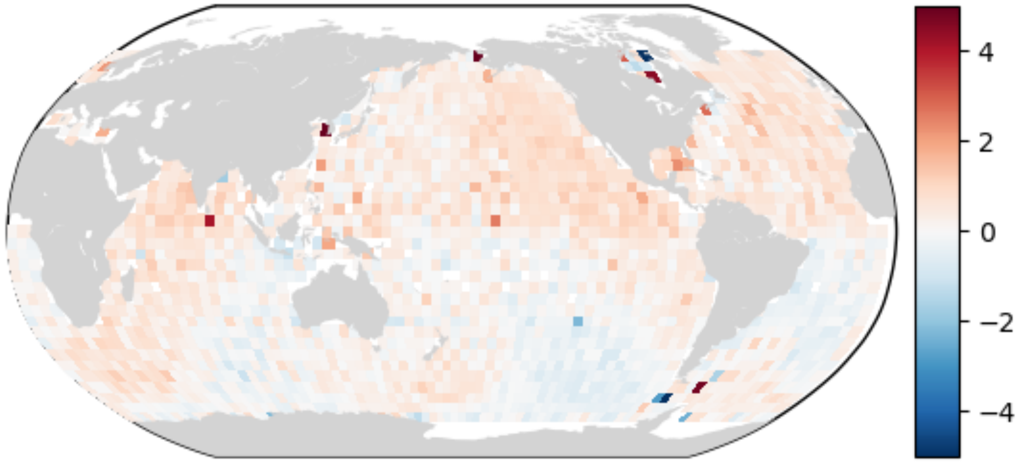

Difference wrt Xover mean MGDR-B [cm]

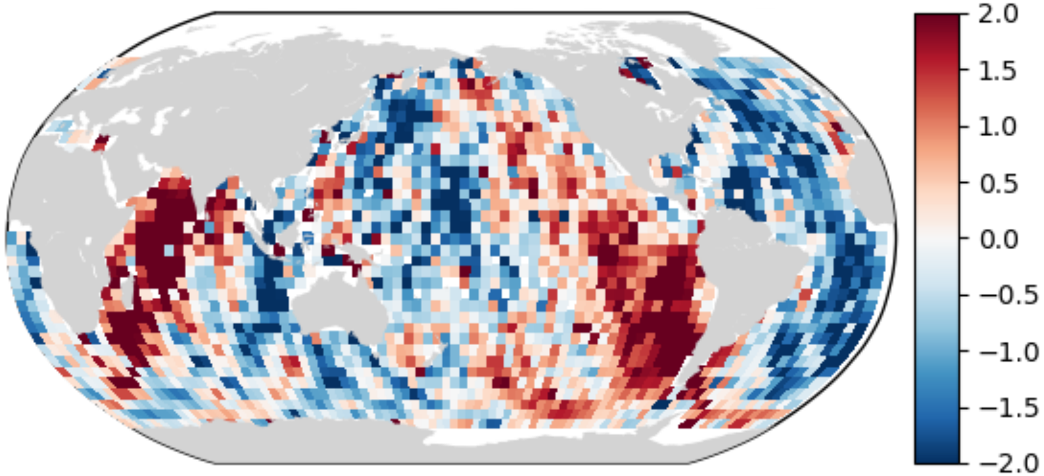

Difference wrt previous solution [cm]

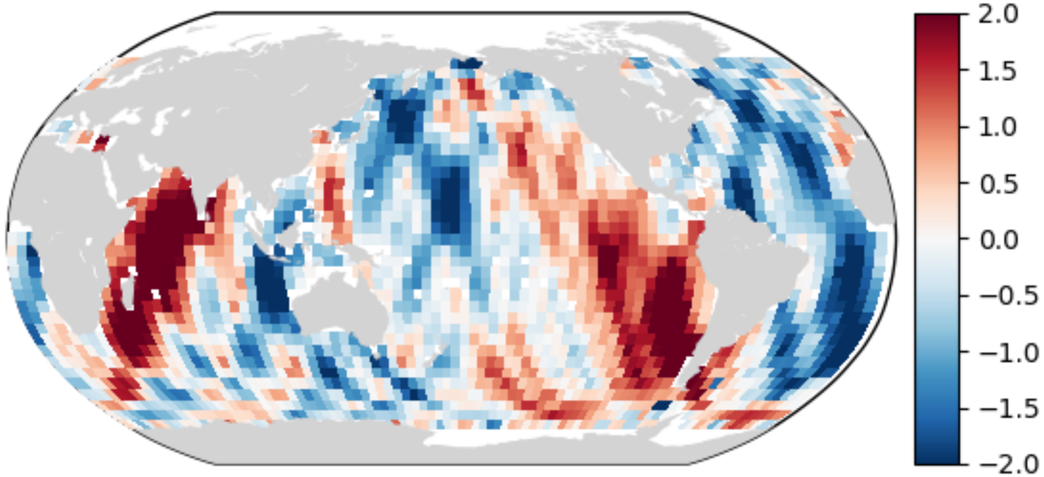

Difference wrt Xover mean GDR-F [cm]

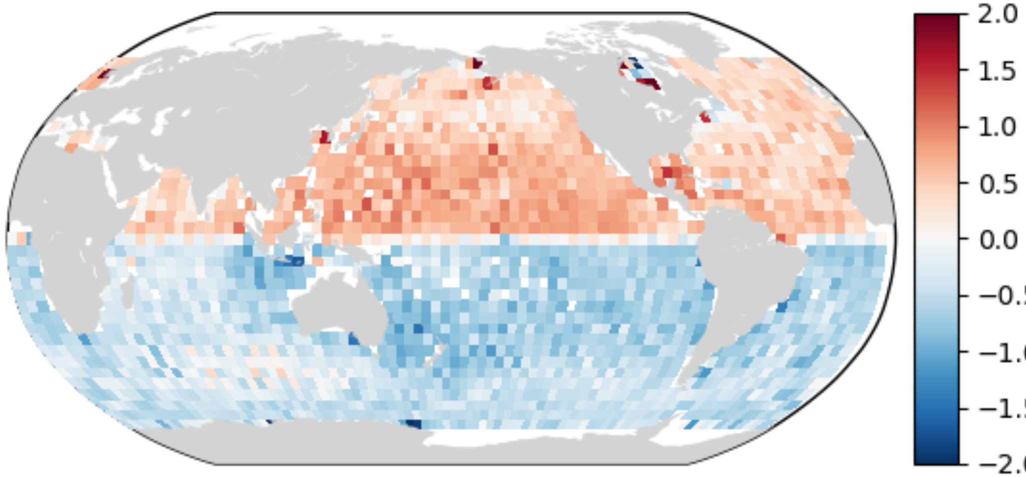

Adding GDR-F: **Dry tropo**

Xover mean of intermediary SSHA solution [cm]

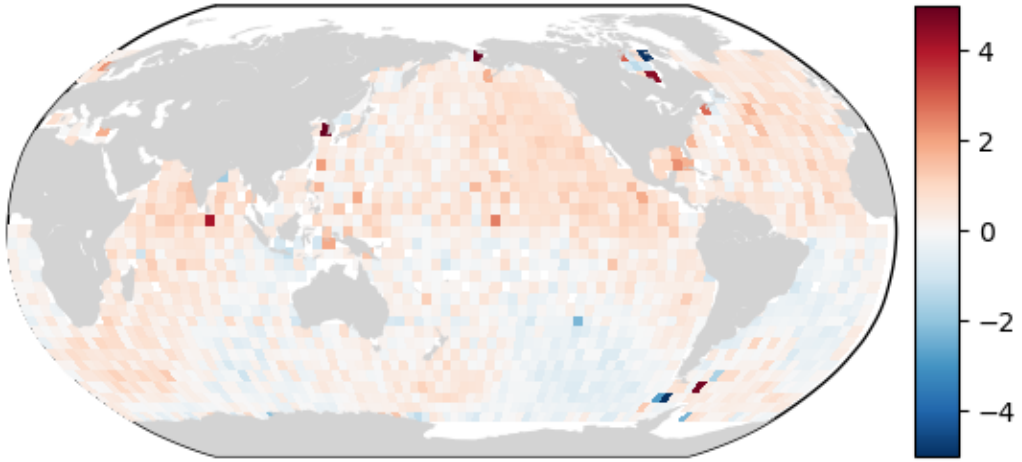

Difference wrt Xover mean MGDR-B [cm]

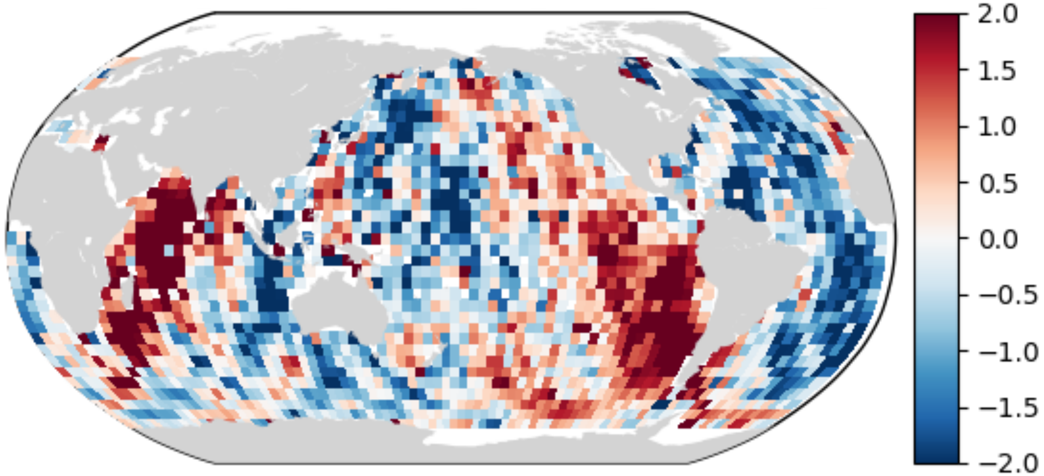

Difference wrt previous solution [cm]

Difference wrt Xover mean GDR-F [cm]

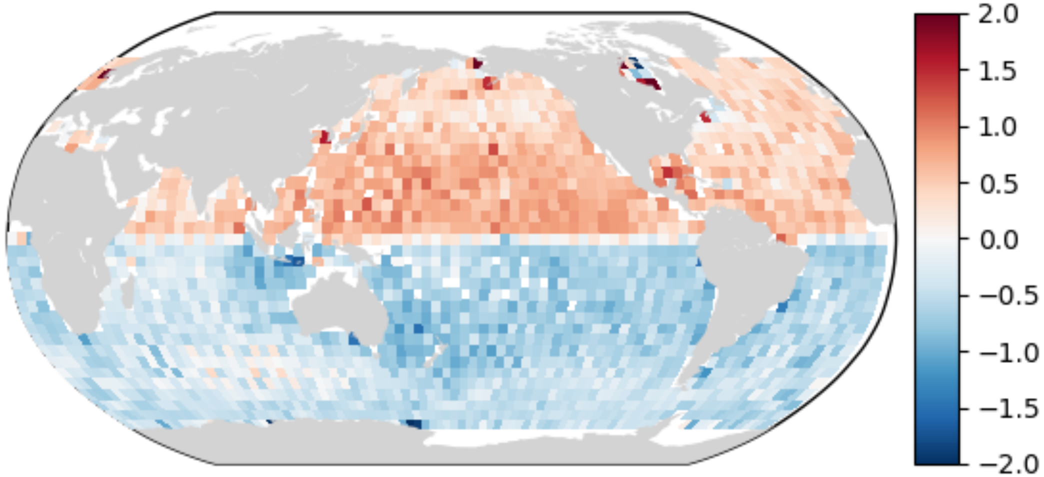

Adding GDR-F: **Radiometer wet path delay**

Side-A

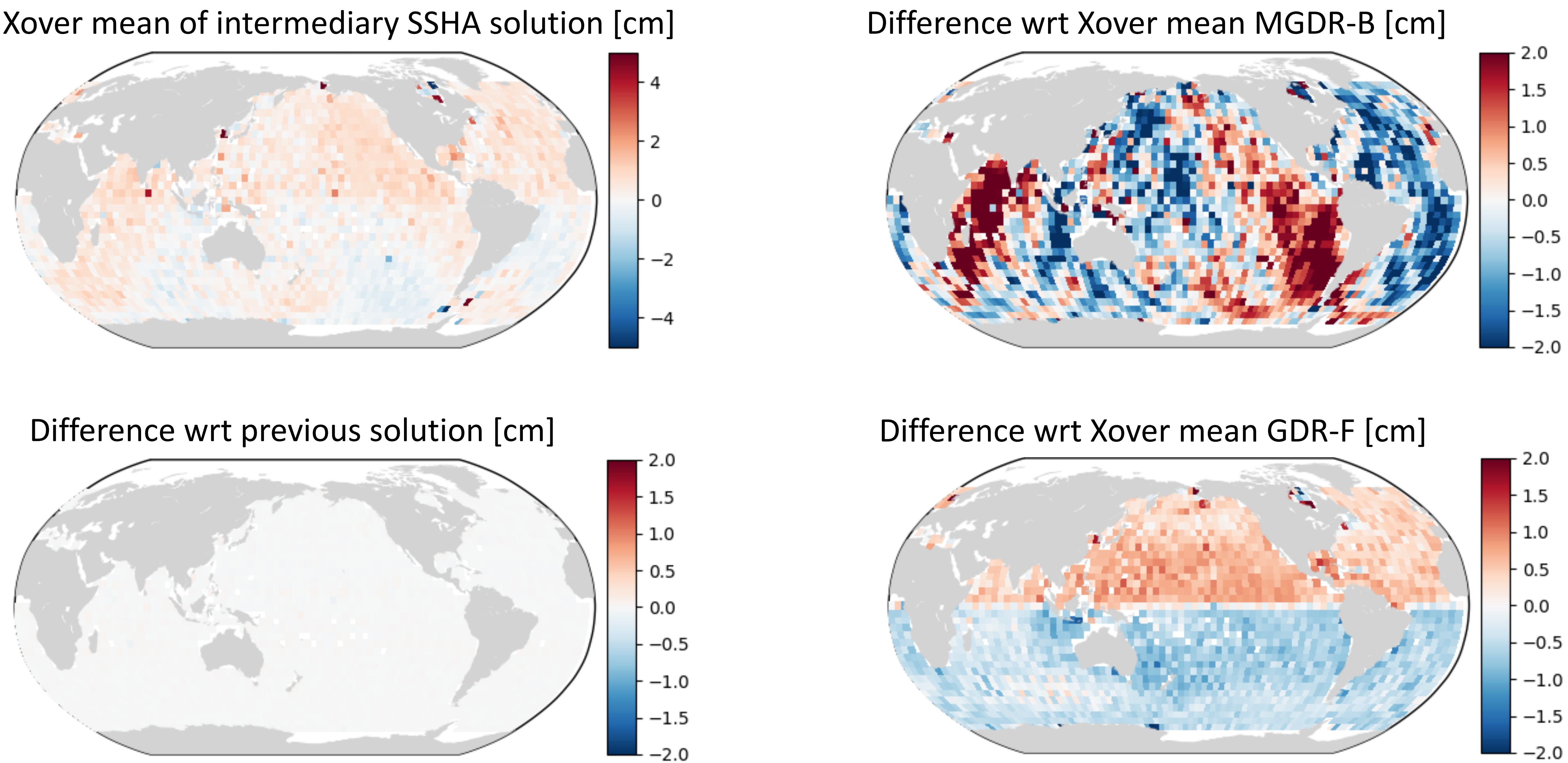

Adding GDR-F: **Sea state bias (Putnam et al., OSTST 2020)**

Xover mean of intermediary SSHA solution [cm]

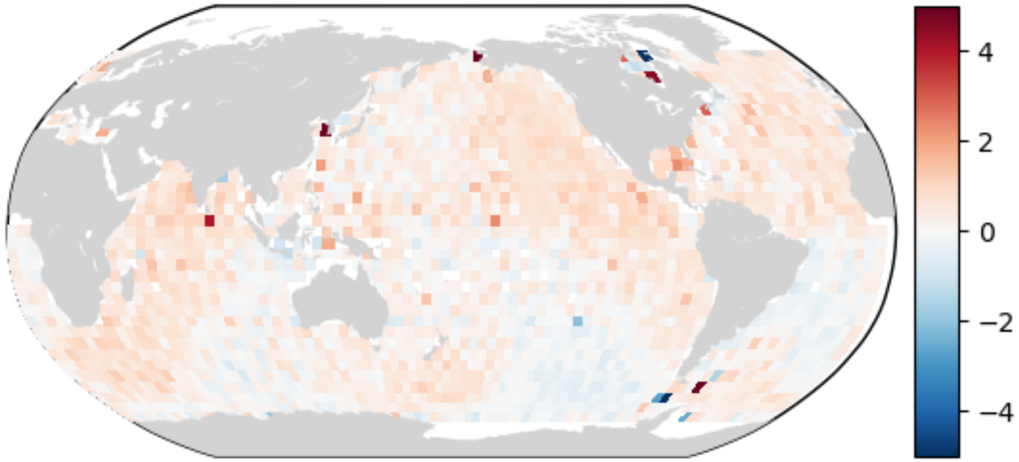

Difference wrt Xover mean MGDR-B [cm]

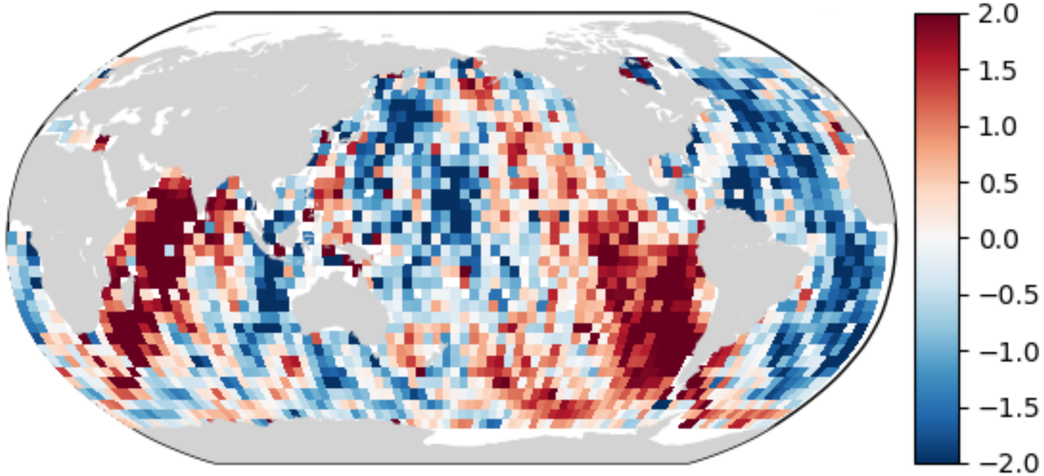

Difference wrt previous solution [cm]

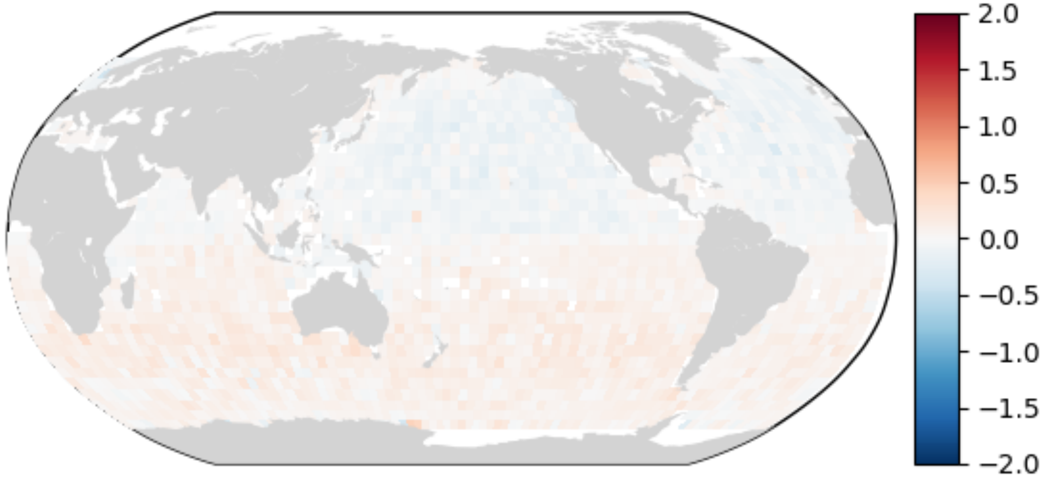

Difference wrt Xover mean GDR-F [cm]

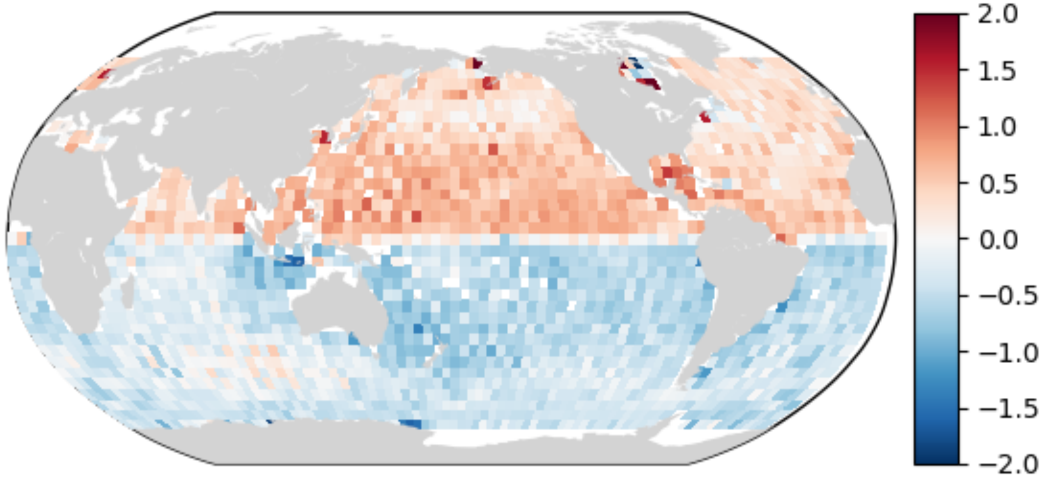

Adding GDR-F: **Ionospheric correction**

Xover mean of intermediary SSHA solution [cm]

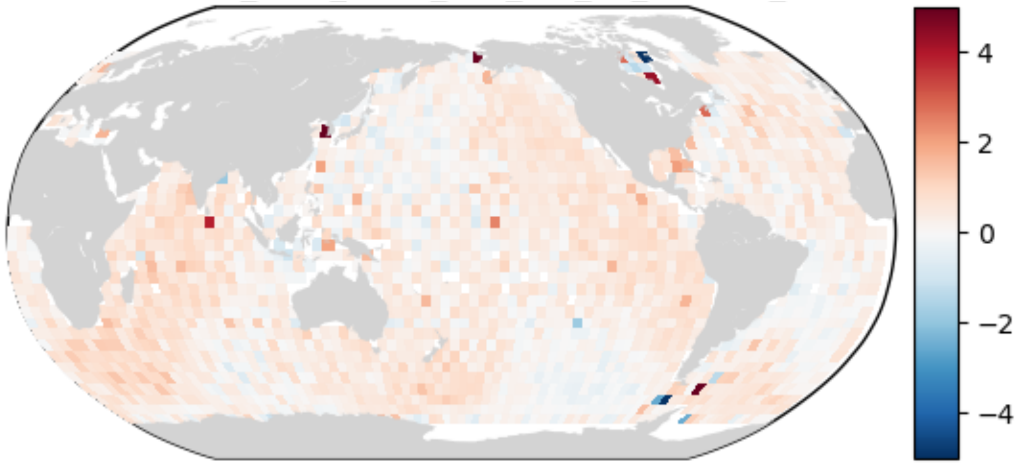

Difference wrt Xover mean MGDR-B [cm]

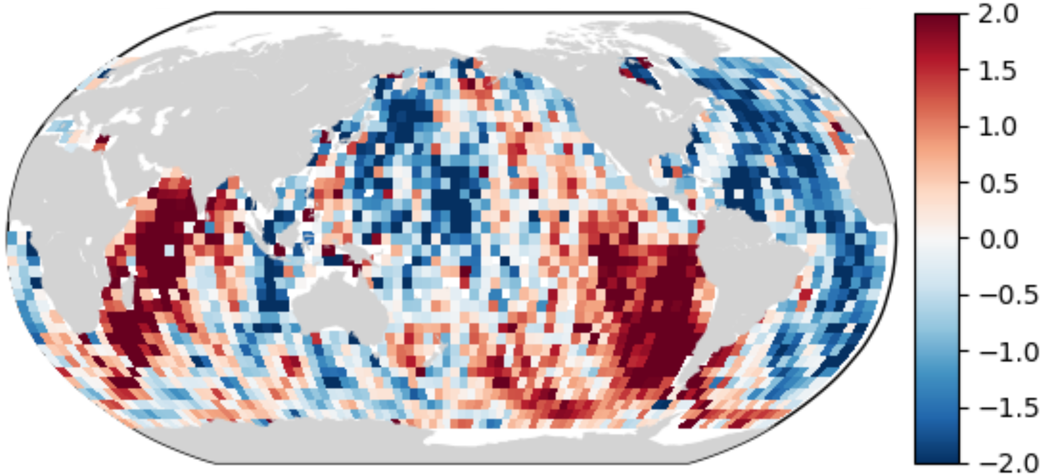

Difference wrt previous solution [cm]

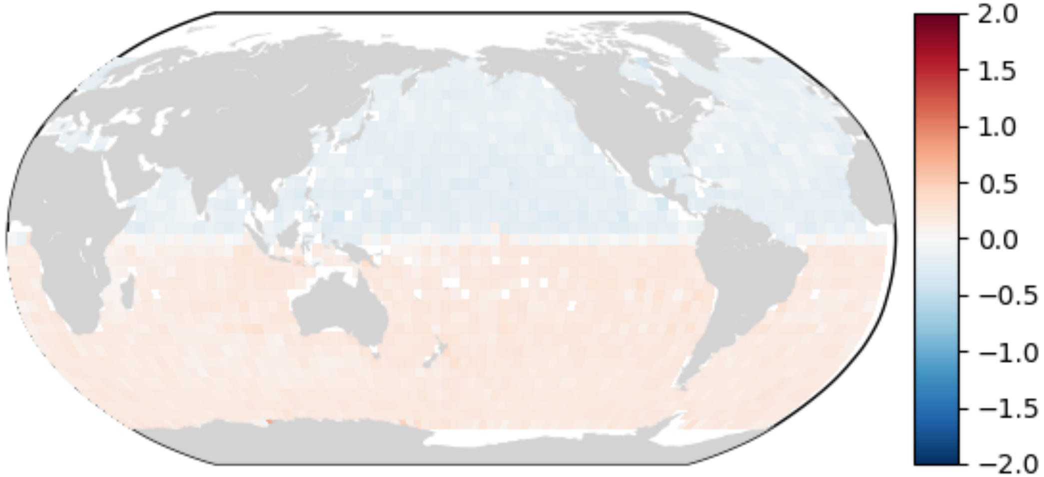

Difference wrt Xover mean GDR-F [cm]

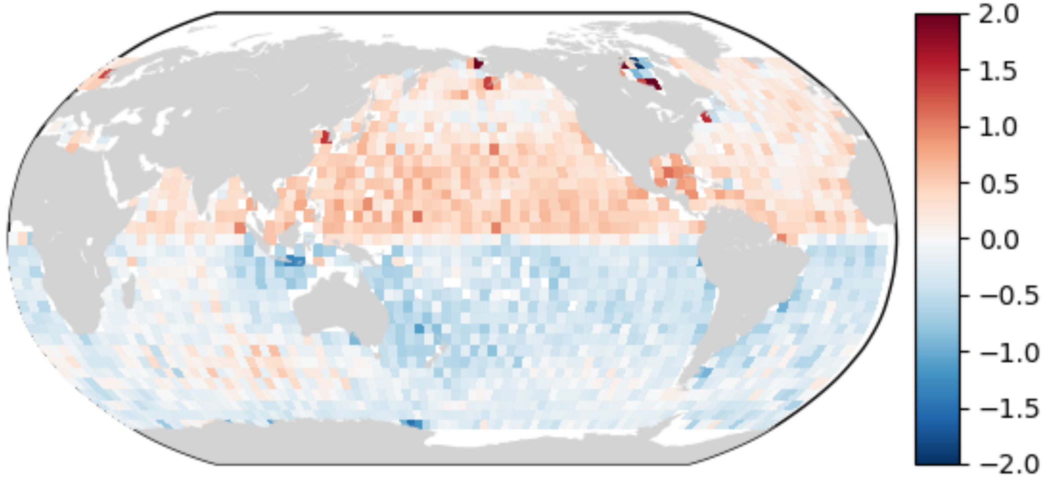

Adding GDR-F: **Numerically retracked range (Desjonquères et al., OSTST 2019)**

Side-A

Xover mean of intermediary SSHA solution [cm]

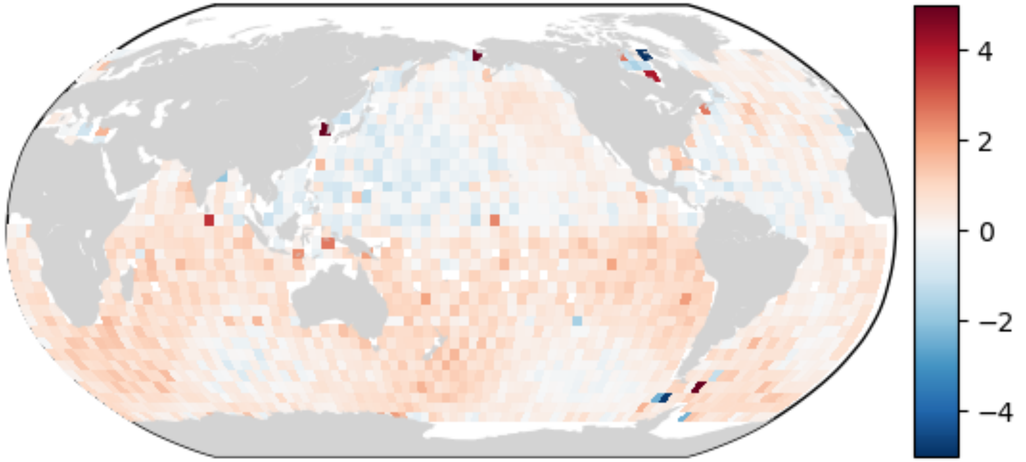

Difference wrt Xover mean MGDR-B [cm]

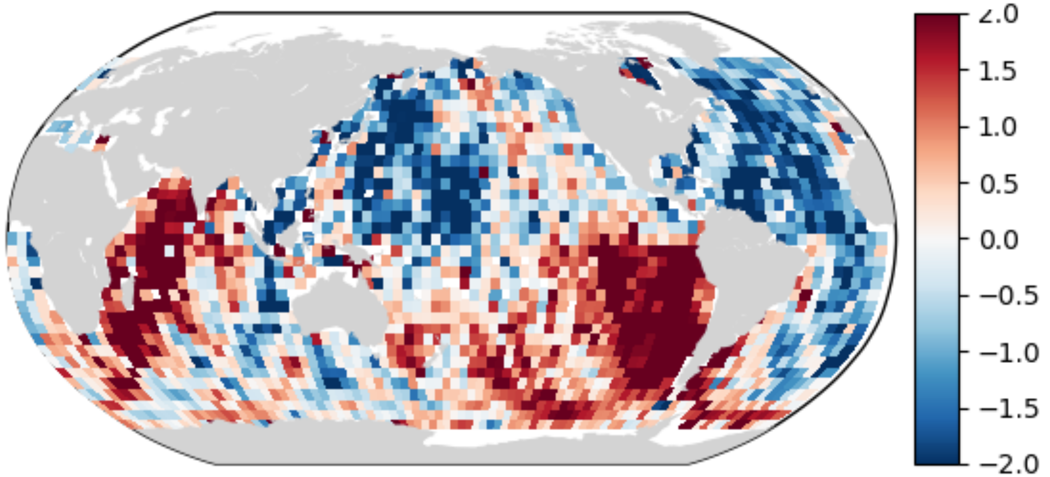

Difference wrt previous solution [cm]

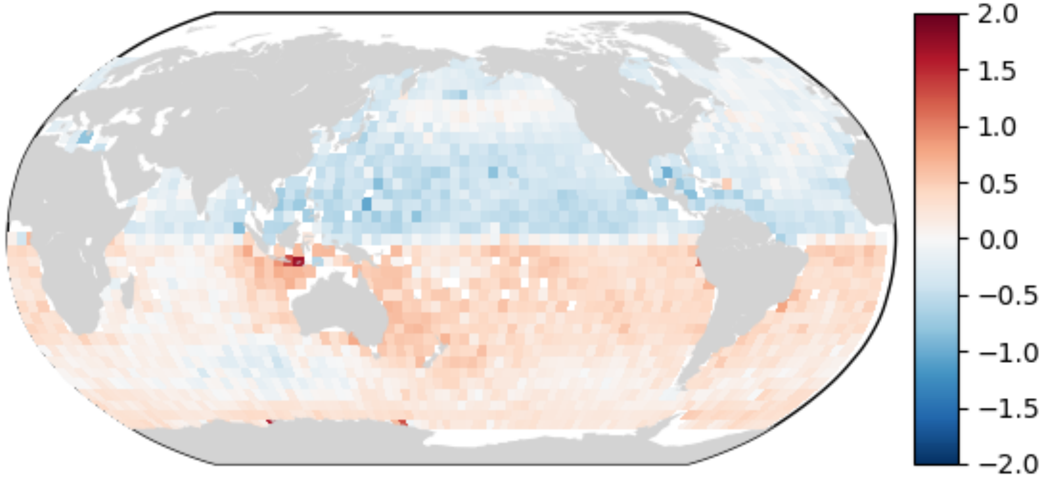

Difference wrt Xover mean GDR-F [cm]

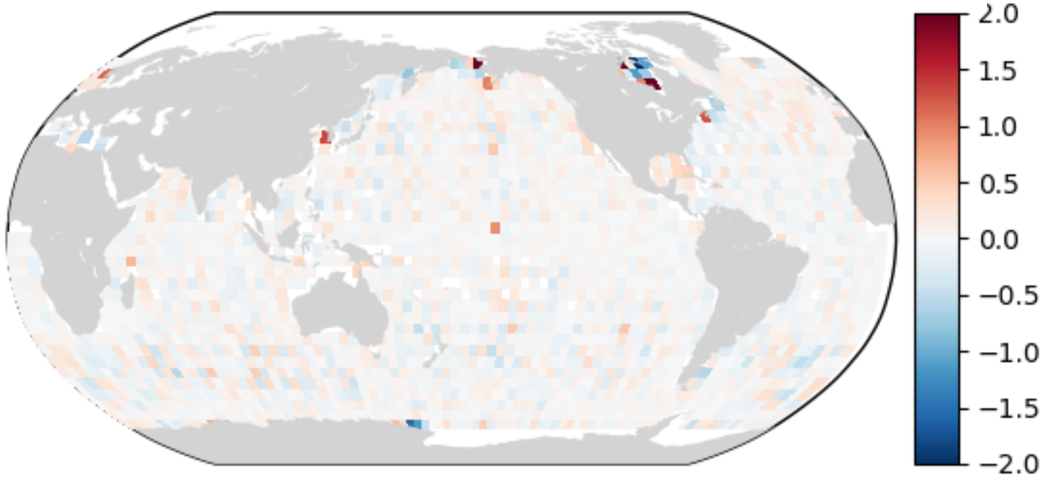

Adding GDR-F: **Internal tide, HF fluct., non-equil. ocean tide**

Xover mean of intermediary SSHA solution [cm]

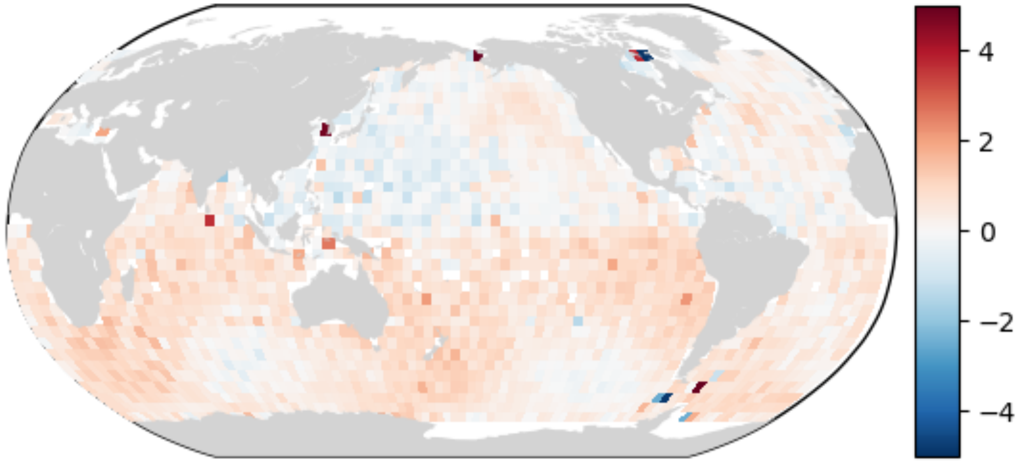

Difference wrt Xover mean MGDR-B [cm]

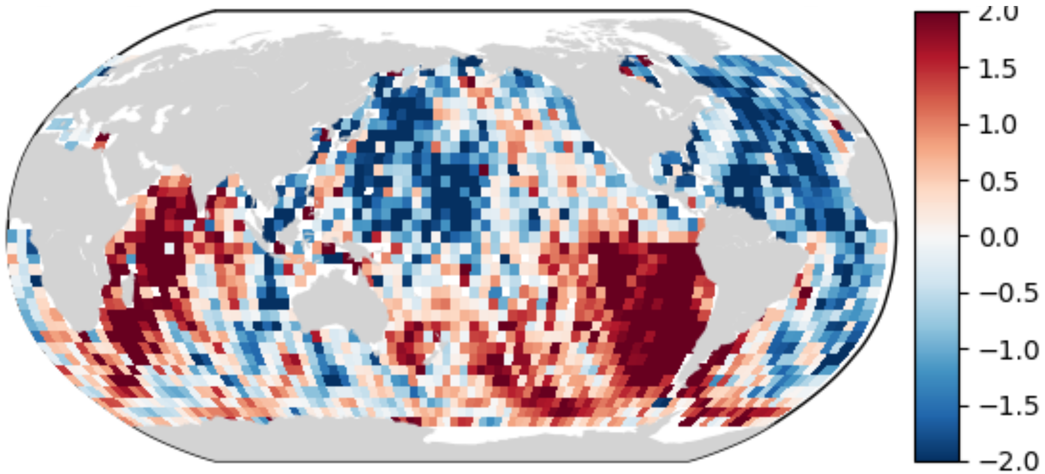

Difference wrt previous solution [cm]

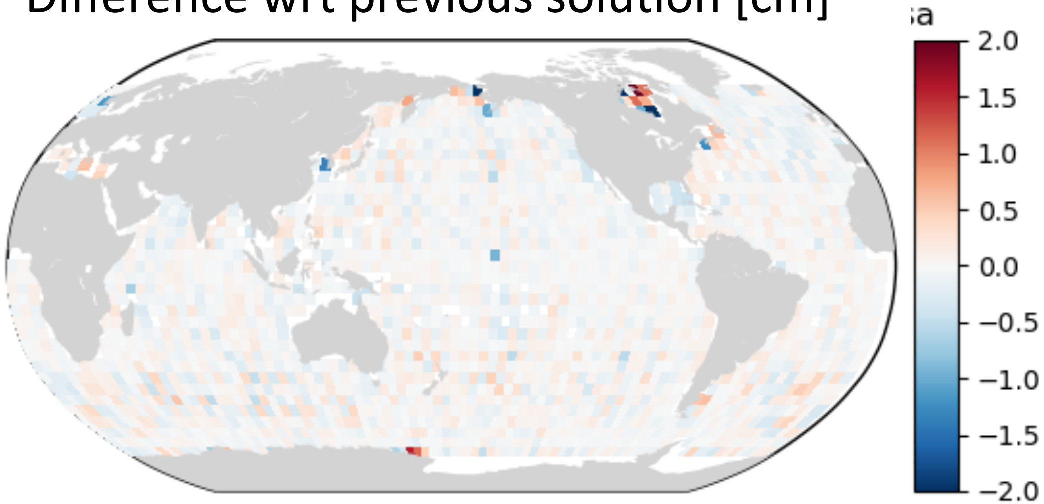

Difference wrt Xover mean GDR-F [cm]

The maps of mean SSHA crossovers show smaller geographically-correlated errors in GDR-F.

Side-B

Xover mean of MGDR-B [cm]

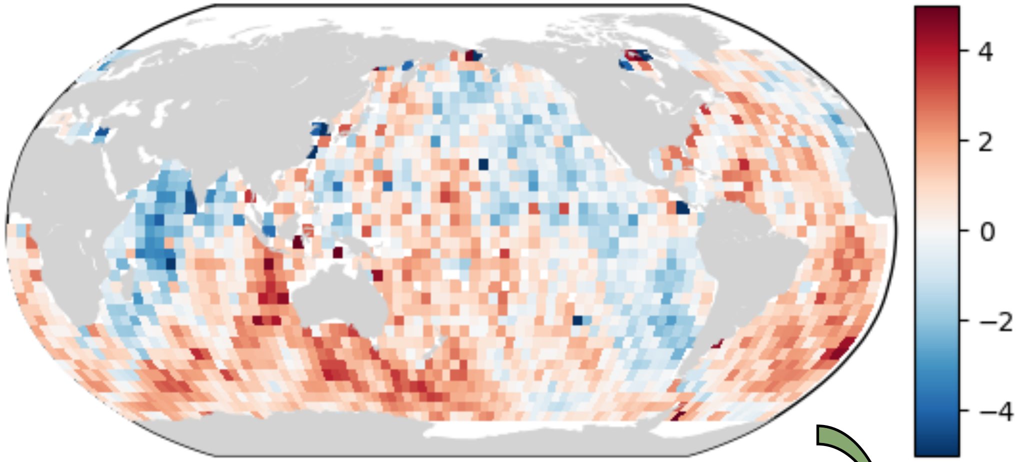

Xover mean of GDR-F [cm]

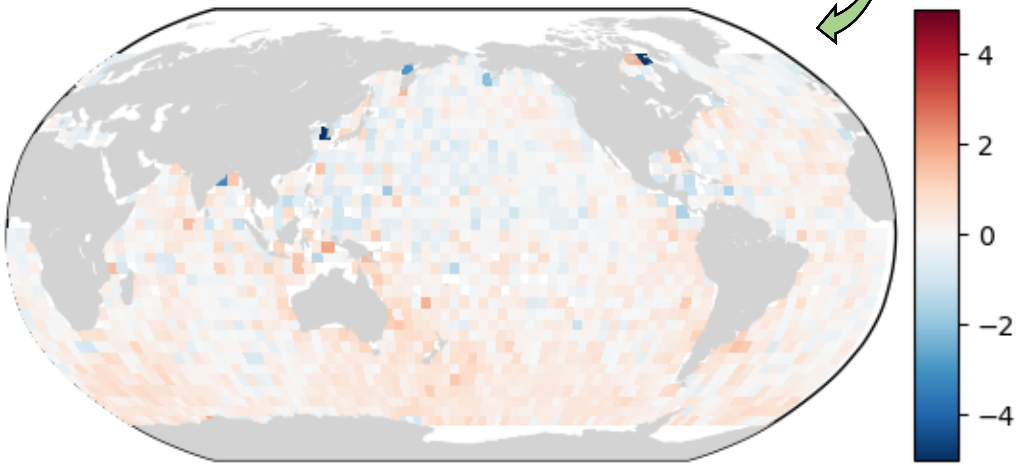

Starting solution is MGDR-B

Xover mean of intermediary SSHA solution [cm]

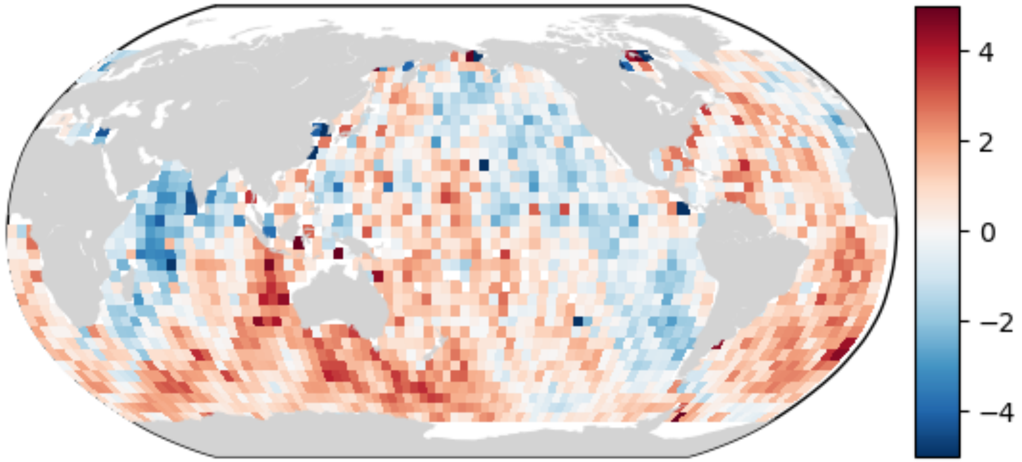

Difference wrt Xover mean MGDR-B [cm]

Difference wrt previous solution [cm]

NA

Difference wrt Xover mean GDR-F [cm]

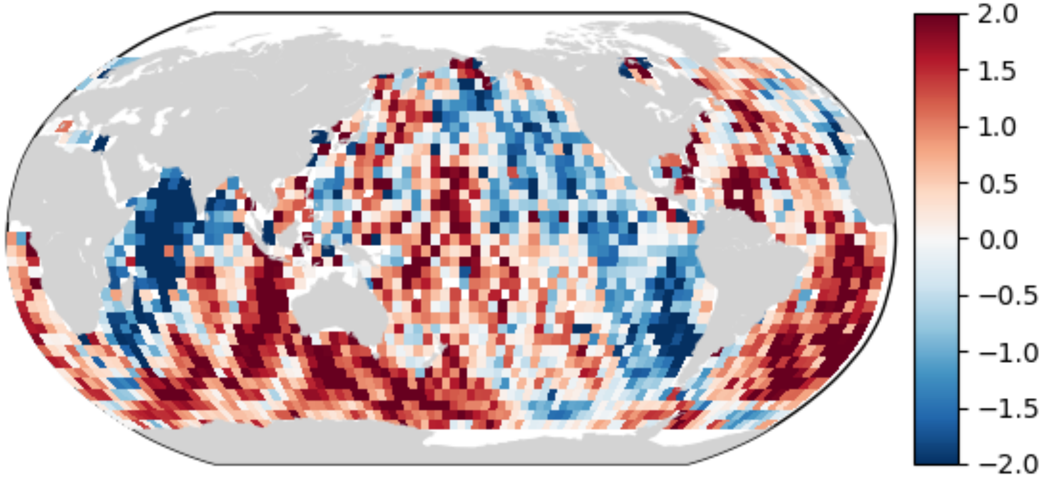

Adding GDR-F: **Geophysical models (pole, solid earth, ocean tides and MSS)**

Xover mean of intermediary SSHA solution [cm]

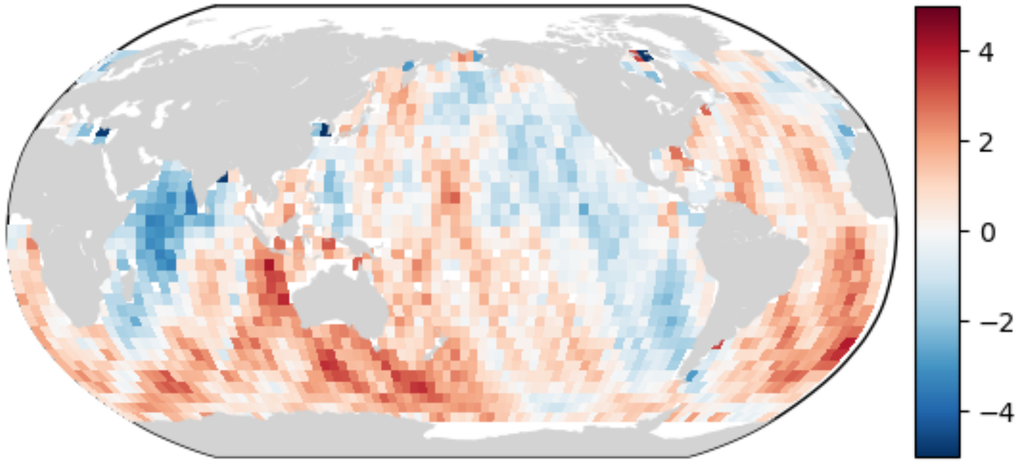

Difference wrt Xover mean MGDR-B [cm]

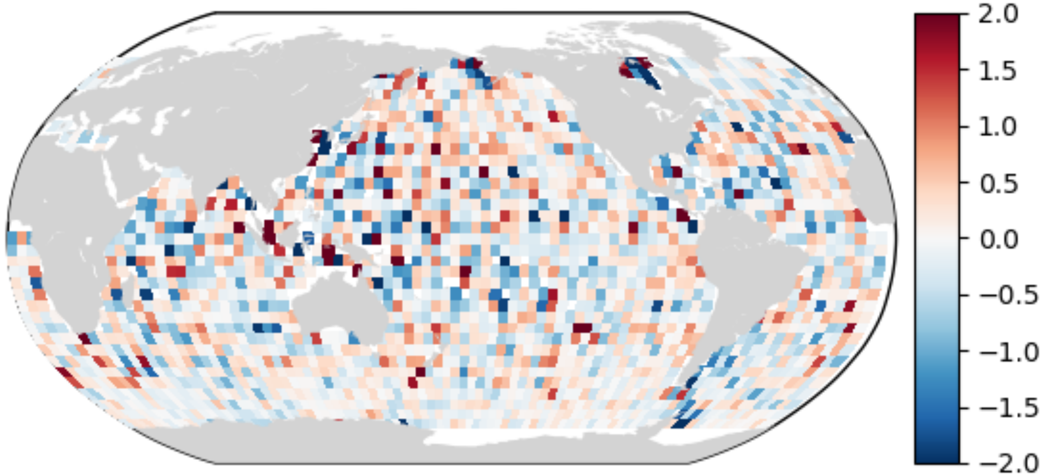

Difference wrt previous solution [cm]

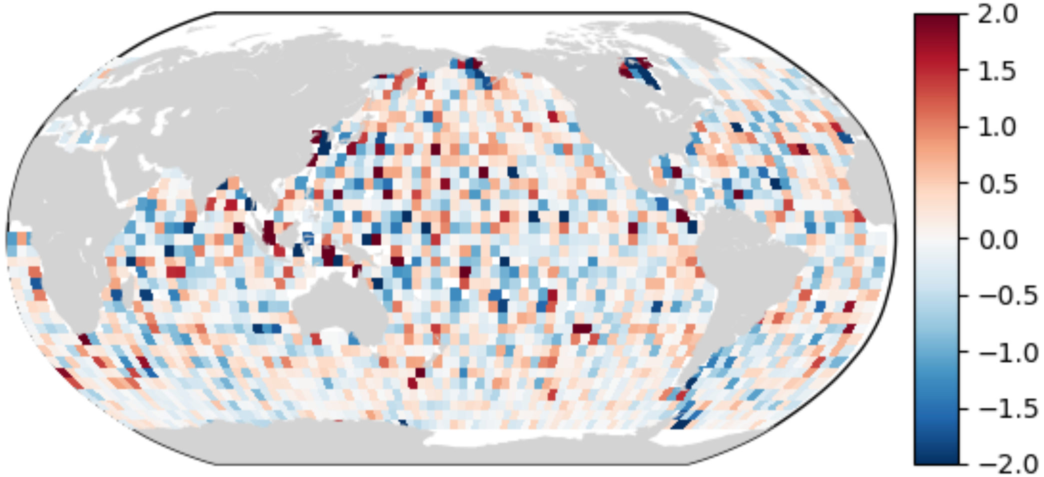

Difference wrt Xover mean GDR-F [cm]

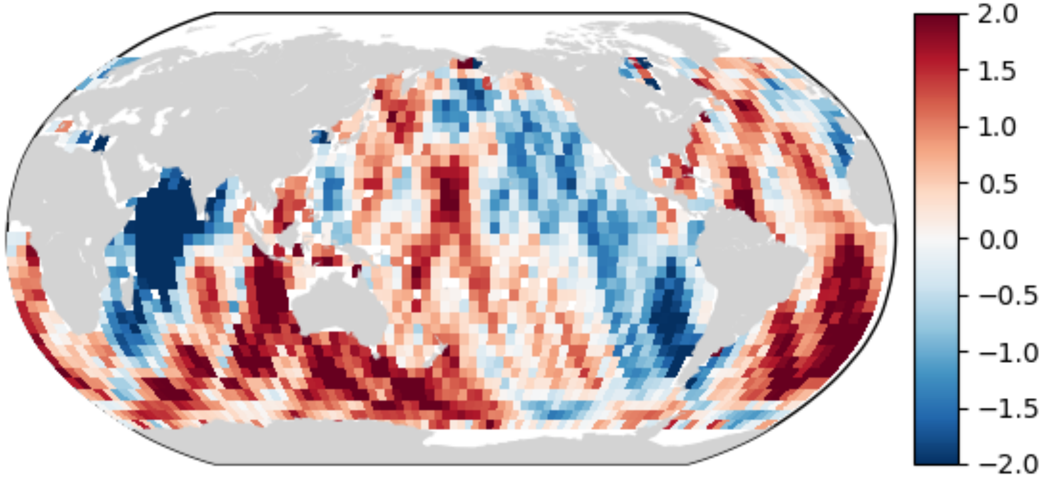

Adding GDR-F: **Orbit (GSFC)**

Xover mean of intermediary SSHA solution [cm]

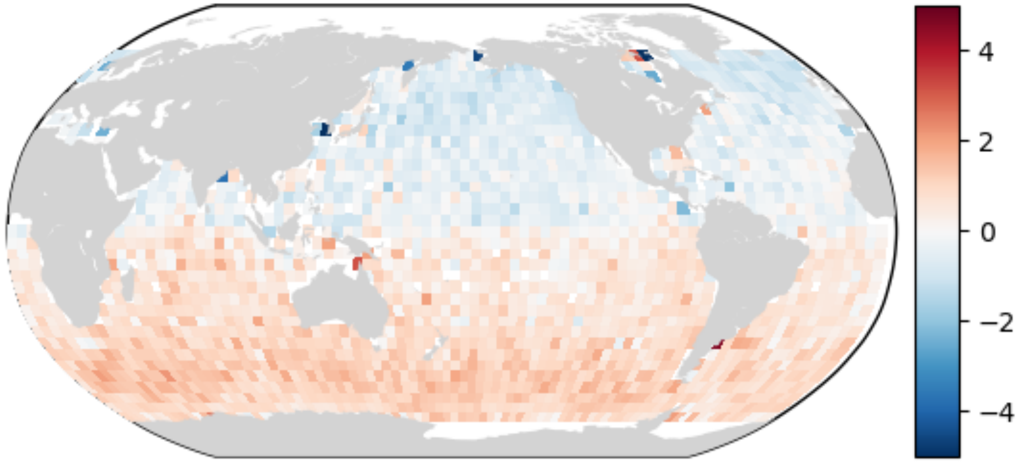

Difference wrt Xover mean MGDR-B [cm]

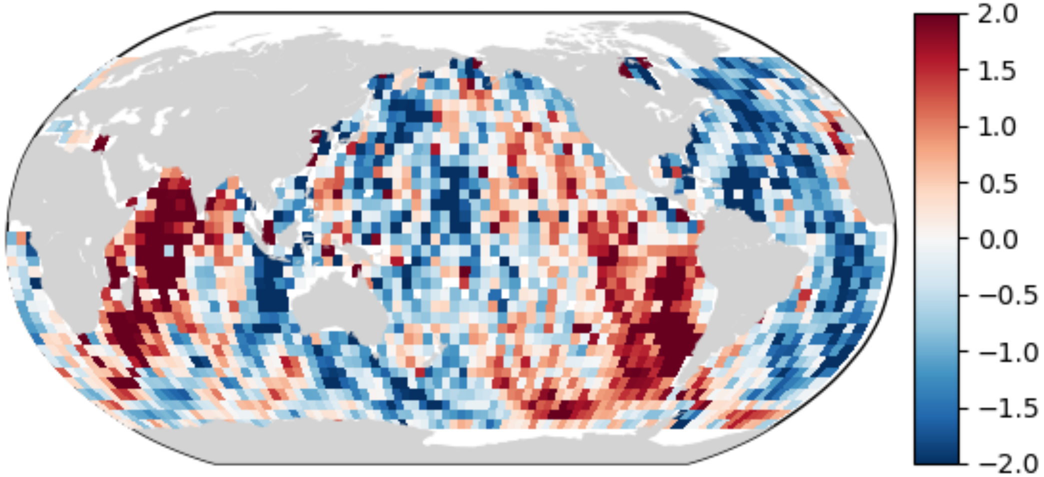

Difference wrt previous solution [cm]

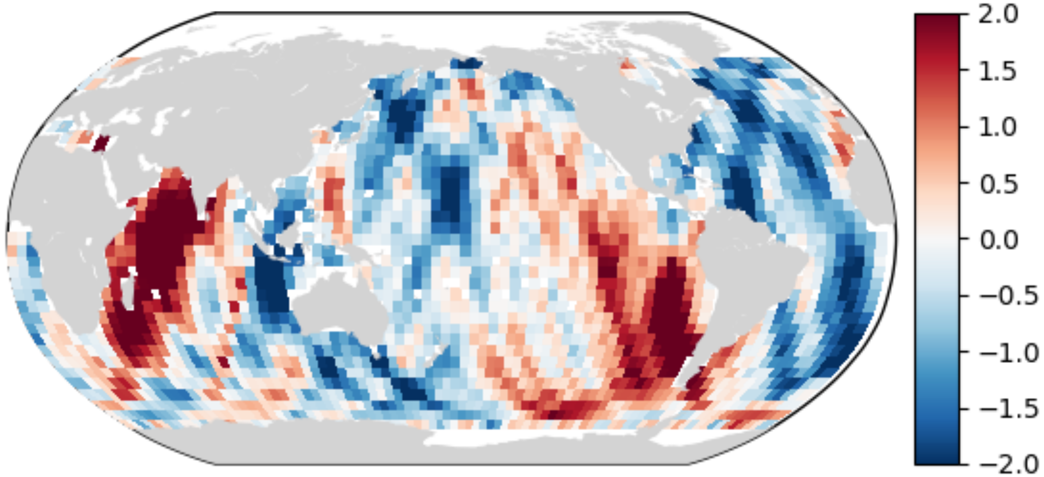

Difference wrt Xover mean GDR-F [cm]

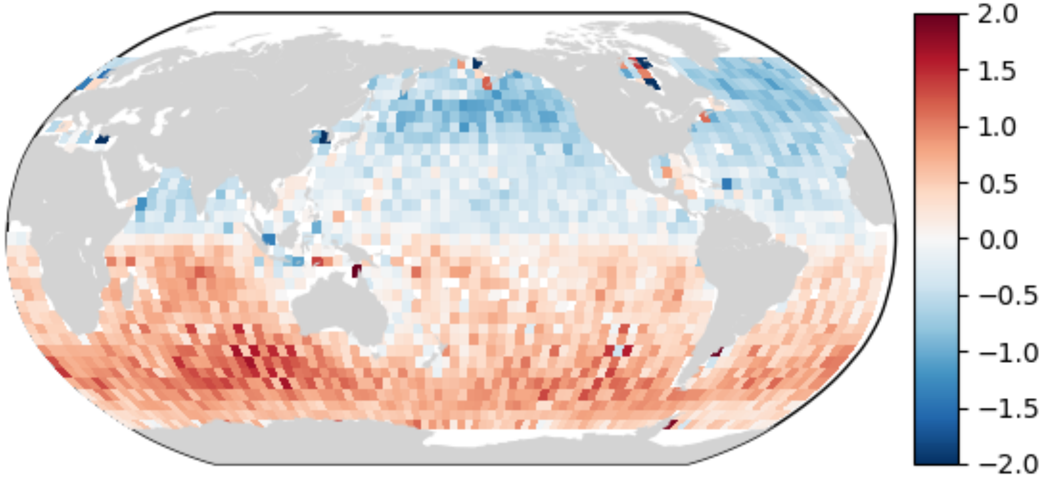

Adding GDR-F: **Dry tropo**

Xover mean of intermediary SSHA solution [cm]

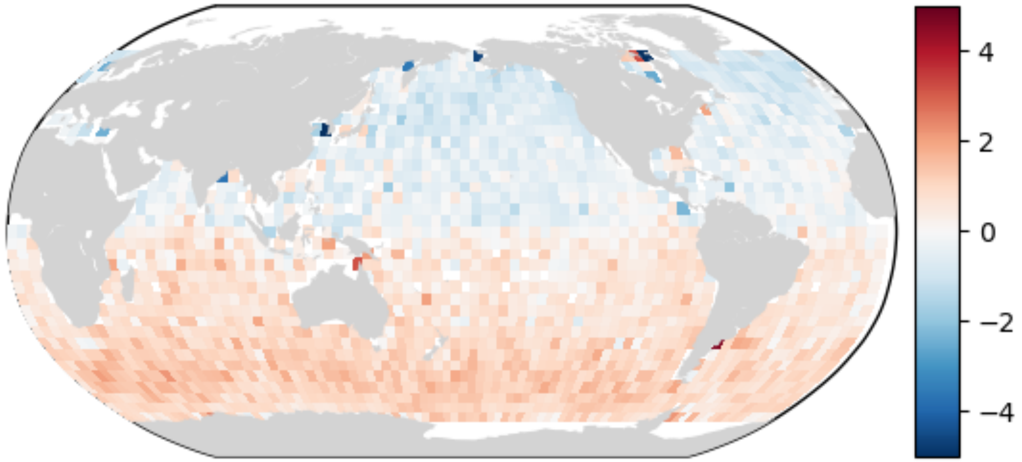

Difference wrt Xover mean MGDR-B [cm]

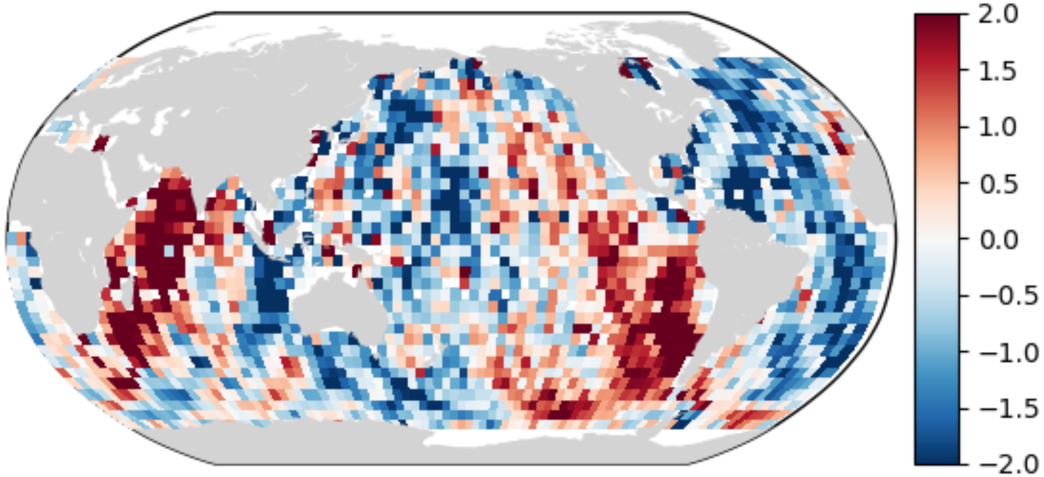

Difference wrt previous solution [cm]

Difference wrt Xover mean GDR-F [cm]

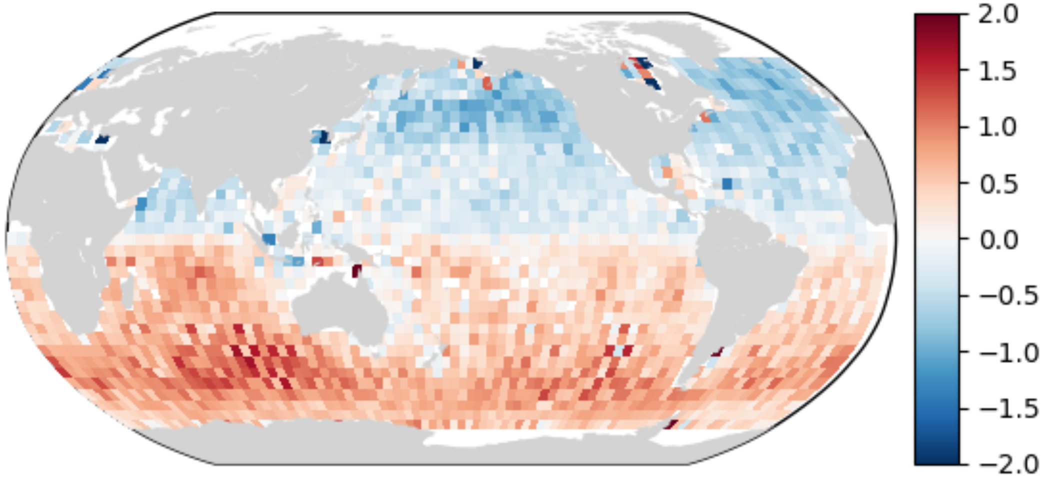

Adding GDR-F: **Radiometer wet path delay**

Xover mean of intermediary SSHA solution [cm]

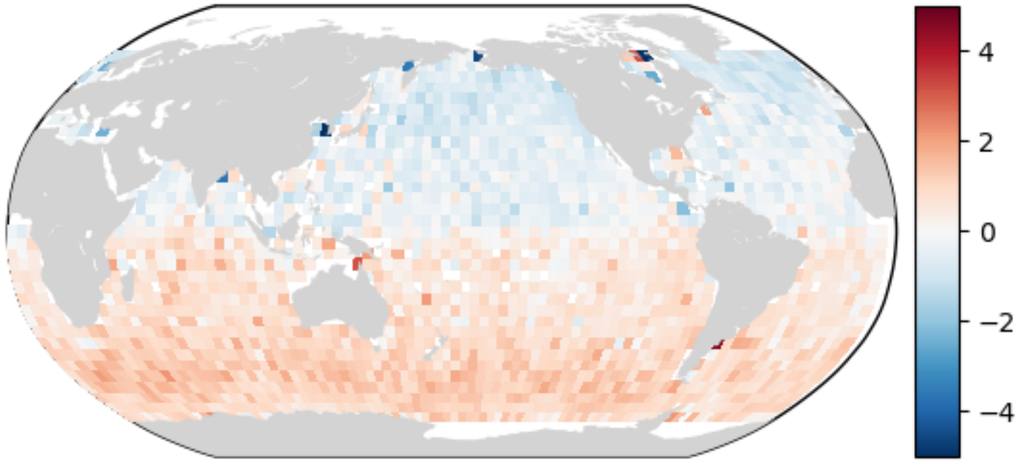

Difference wrt Xover mean MGDR-B [cm]

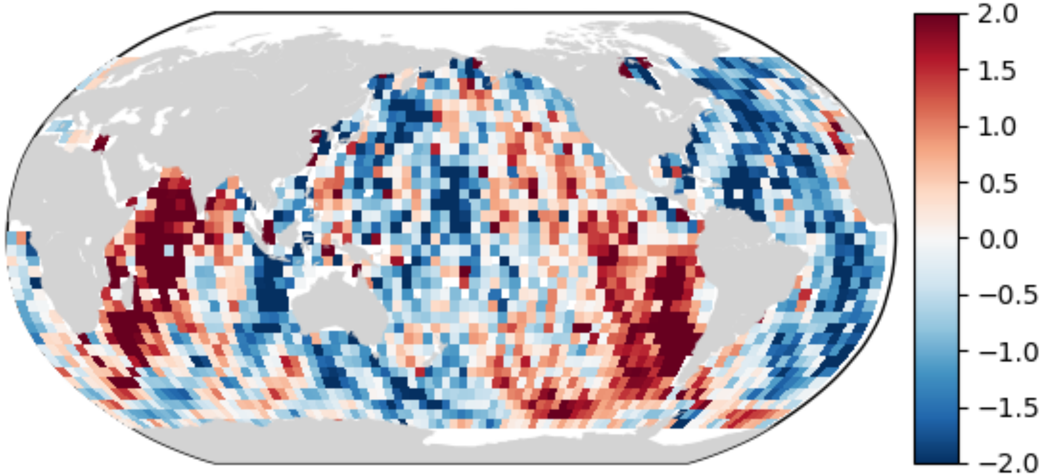

Difference wrt previous solution [cm]

Difference wrt Xover mean GDR-F [cm]

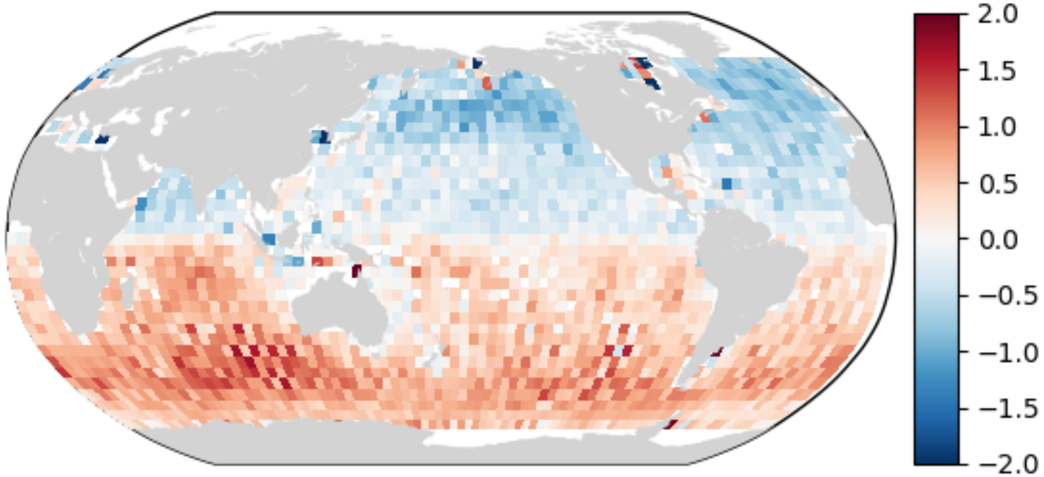

Adding GDR-F: **Sea state bias (Putnam et al., OSTST 2020)**

Xover mean of intermediary SSHA solution [cm]

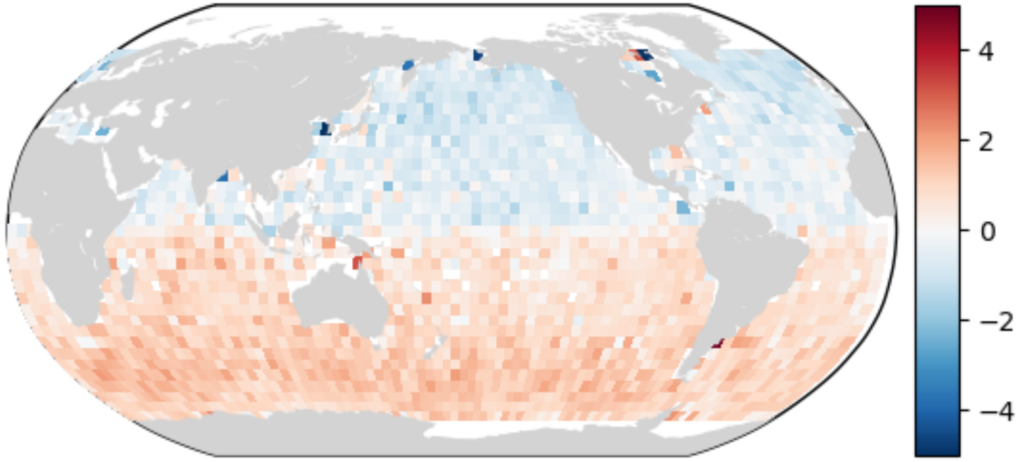

Difference wrt Xover mean MGDR-B [cm]

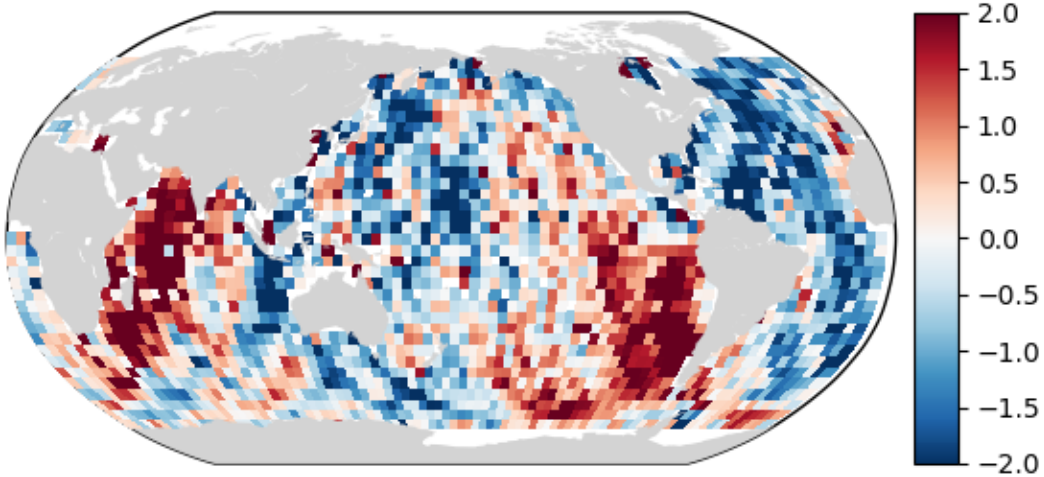

Difference wrt previous solution [cm]

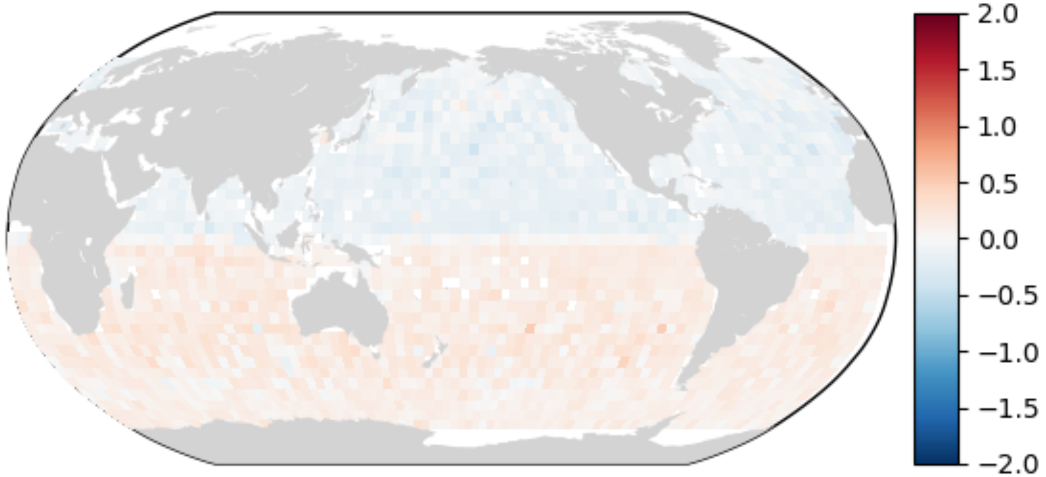

Difference wrt Xover mean GDR-F [cm]

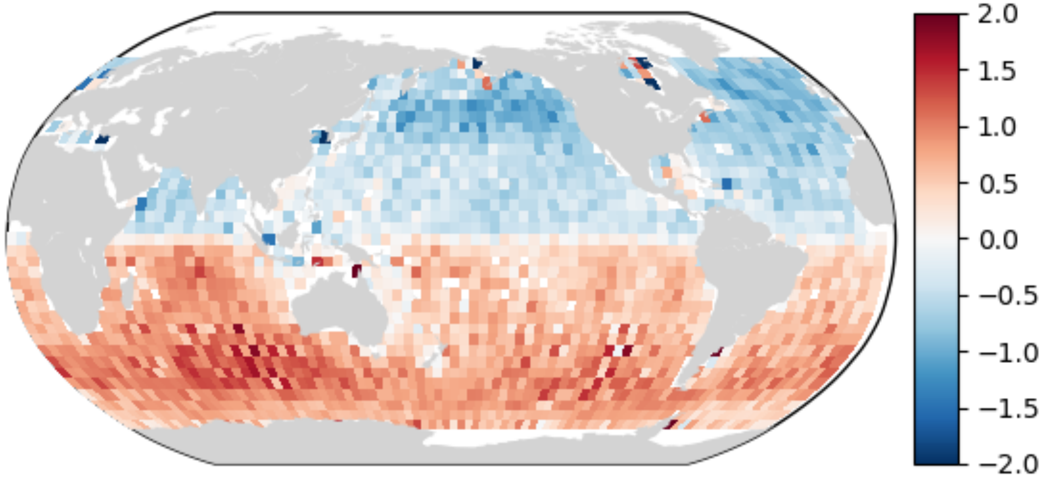

Adding GDR-F: **Ionospheric correction**

Xover mean of intermediary SSHA solution [cm]

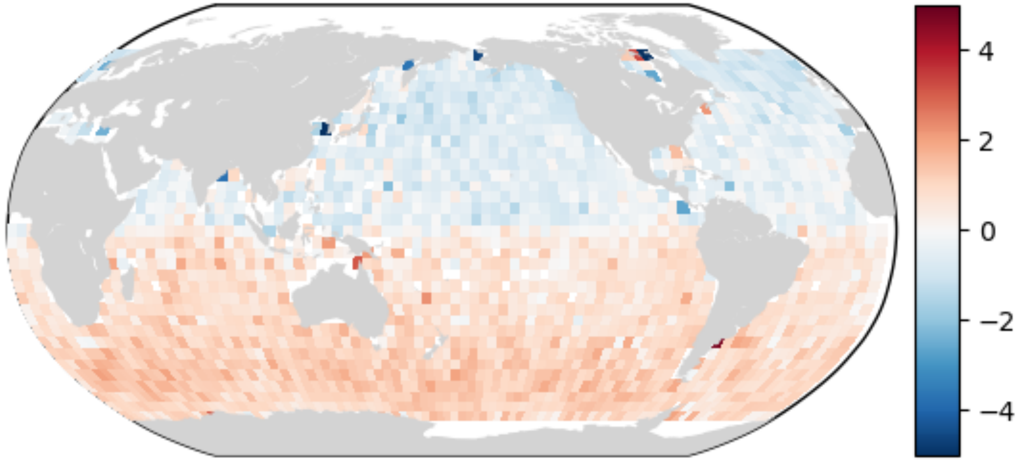

Difference wrt Xover mean MGDR-B [cm]

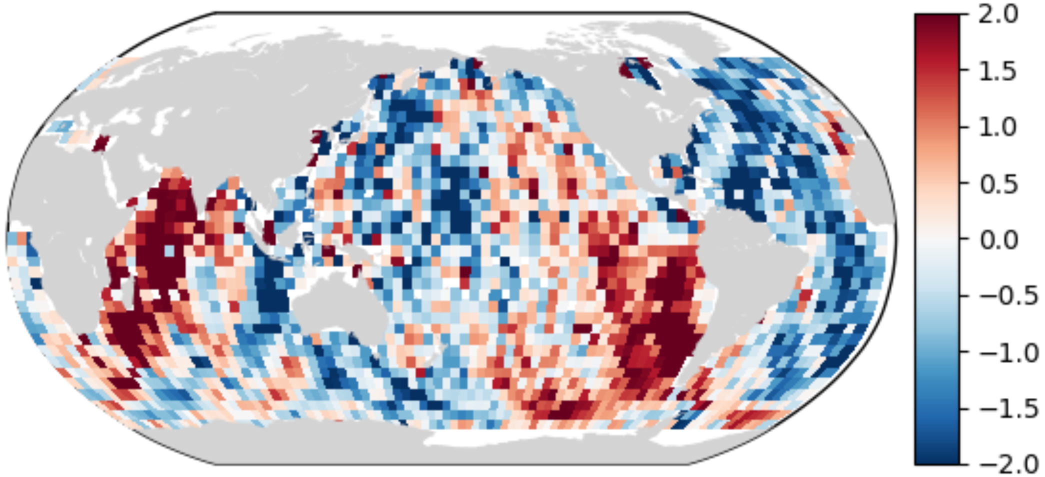

Difference wrt previous solution [cm]

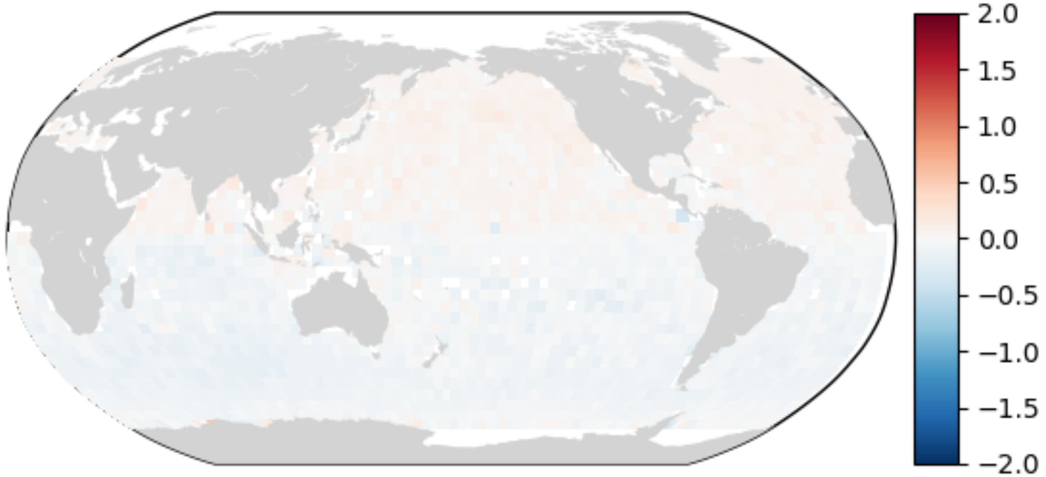

Difference wrt Xover mean GDR-F [cm]

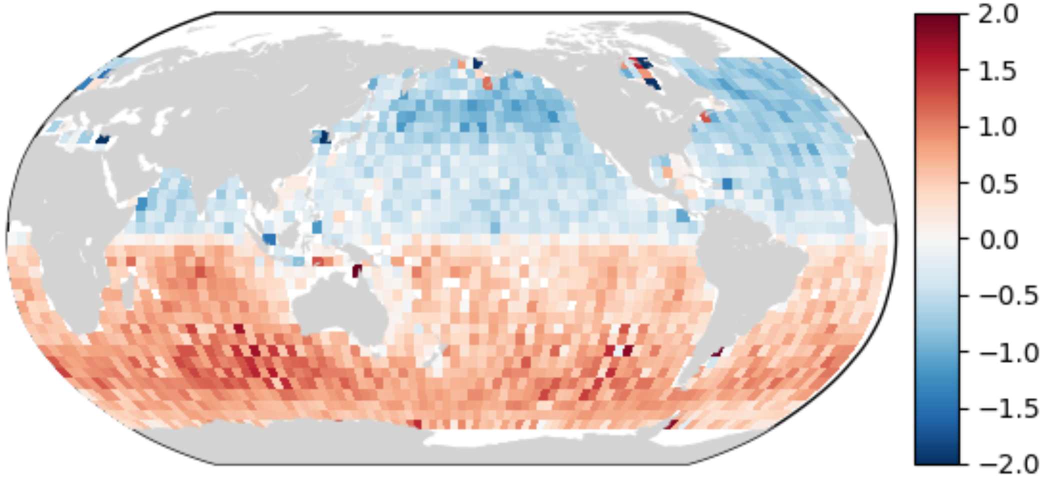

Adding GDR-F: **Numerically retracked range (Desjonquères et al., OSTST 2019)**

Xover mean of intermediary SSHA solution [cm]

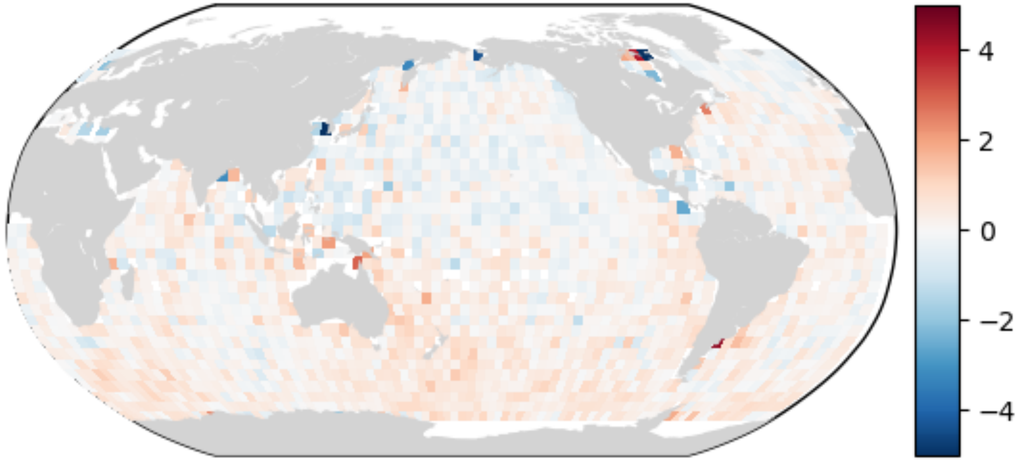

Difference wrt Xover mean MGDR-B [cm]

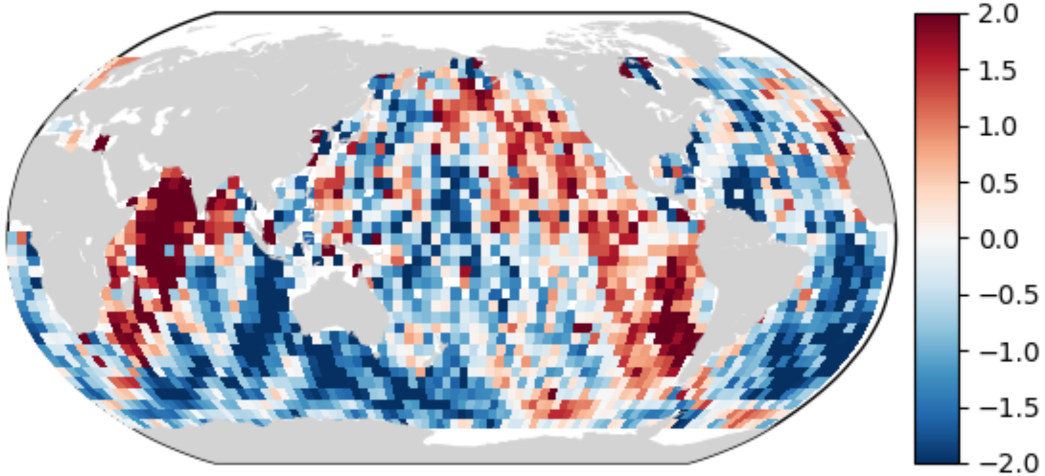

Difference wrt previous solution [cm]

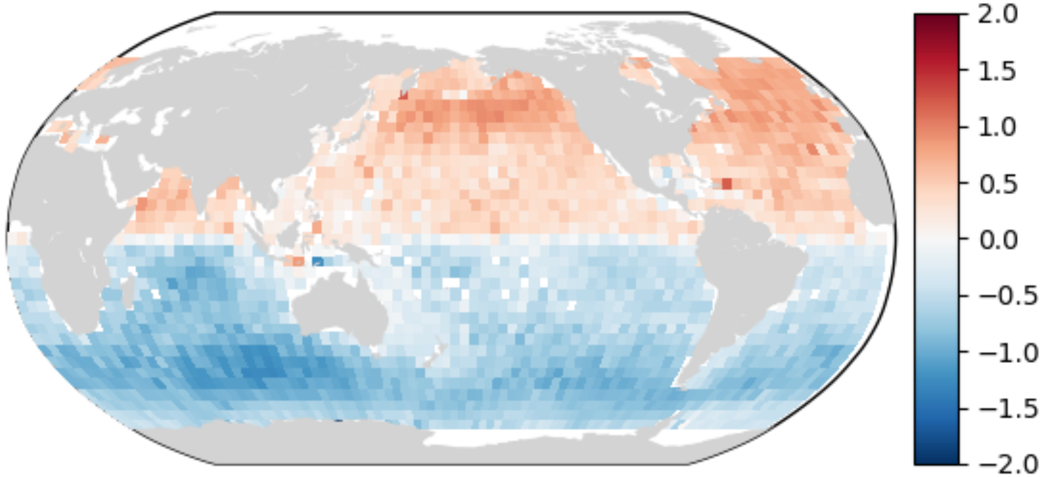

Difference wrt Xover mean GDR-F [cm]

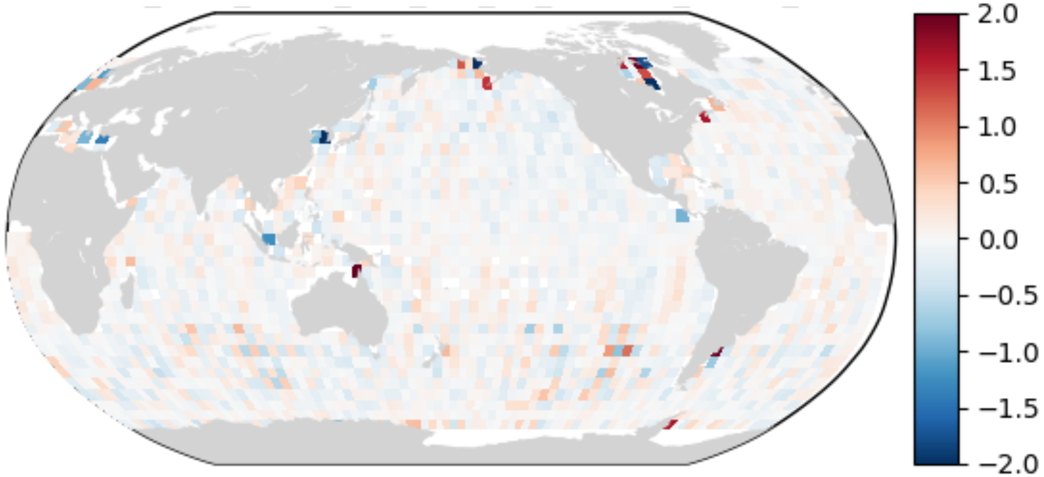

Adding GDR-F: **Internal tide, HF fluct., non-equil. ocean tide**

Xover mean of intermediary SSHA solution [cm]

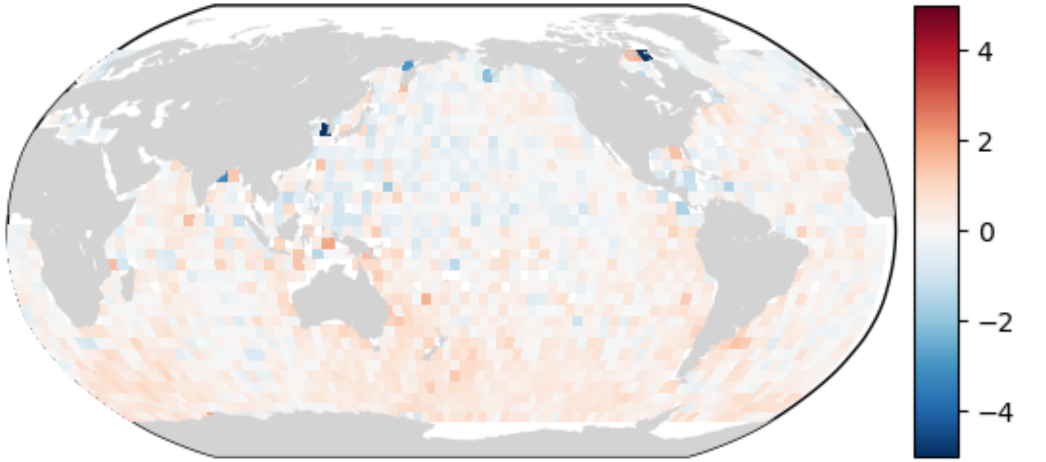

Difference wrt Xover mean MGDR-B [cm]

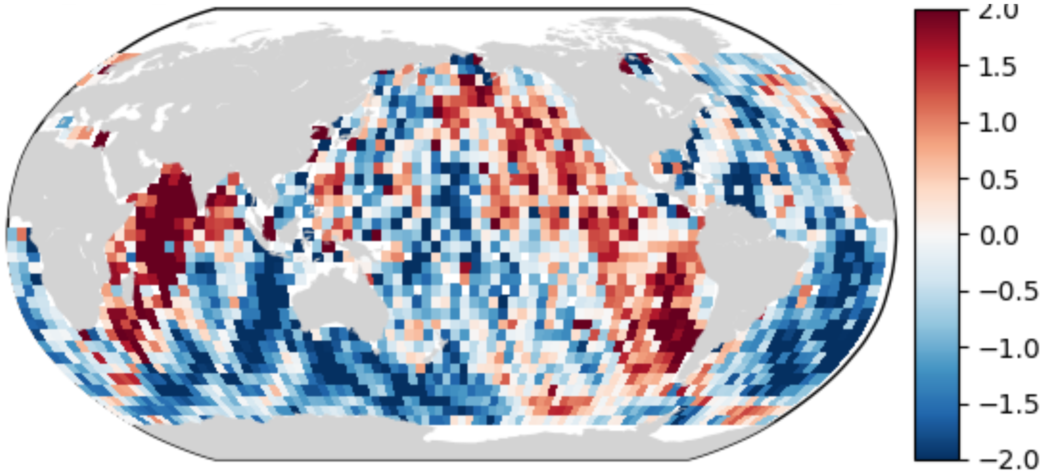

Difference wrt previous solution [cm]

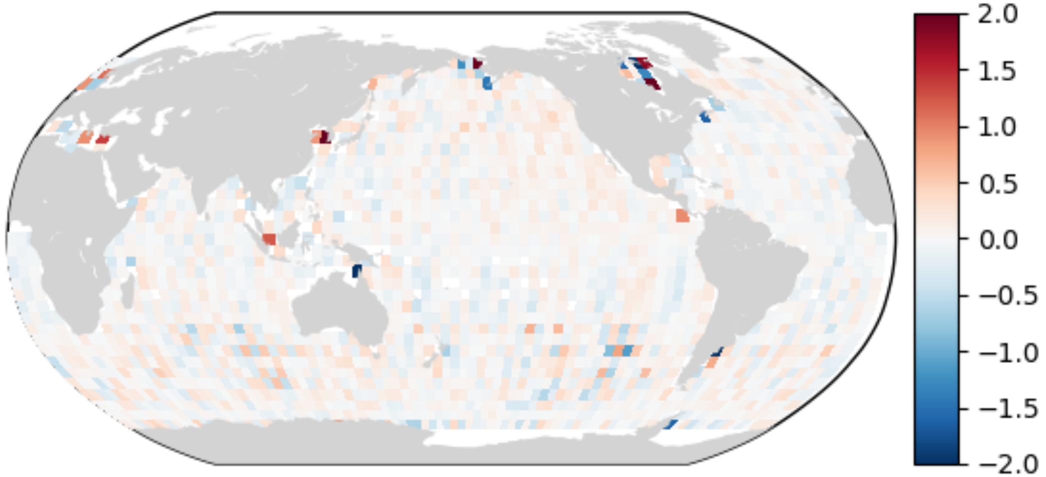

Difference wrt Xover mean GDR-F [cm]

How does each component update influence the final sea surface height anomaly (SSHA)?

1. **The SSHA curve**
   - The updates over side-B are stable in time and stochastic in nature, aside from the atmospheric path delays.
   - In contrast, side-A contains notable systematic differences between MGDR-B and GDR-F. The dominant difference stems from the numerically retracked ranges and reprocessed calibrations, which induce a cm-level, evolving signal (see Desjonquères et al., OSTST 2019). Accordingly, the ionosphere and SSB corrections also contribute several mms to SSHA differences at the end of side-A.
   - The update in geophysical models modifies the SSHA curve by a stochastic signal with an amplitude of ~3 mm.
   - The reprocessed radiometer data corroborate a near-mm/yr drift difference in the wet path delay over side-A.
   - The updated orbit also shows a 3-mm drop over the last 2.5 years of side-A.
   - The new wet and dry tropospheric path delays entail changes of mm-level, 60-day periodic signals.
2. **Timeseries of SSHA crossover RMS**
   - The dominant contributors to lowering variance from MGDR-B to GDR-F are the geophysical models, orbits, and high-frequency fluctuations; SSHA crossover variance is reduced by 437, 275, and 228 mm^2, respectively.
   - In contrast, the wet and dry tropospheric path delays contribute minimally.
3. **Maps of SSHA crossover means**
   - Geographically-correlated errors (GCE) are considerably reduced from MGDR-B (~4 cm) to GDR-F (~1 cm).
   - The orbit update explains a large majority (~3 cm) of the reduction in GCE amplitude.
   - The ~2 cm-level hemispheric bias is greatly attenuated with the update in ranges and associated SSB and ionospheric corrections. The bias essentially disappears in side-B and remains at a mm-level in side-A.
   - The new geophysical models remove cm-level, homogenously-distributed noise.

Summary

- The TOPEX side-A and side-B products have been generated using:
  - Ground retracking (Desjonquères et al, OSTST 2019)
  - Reprocessed TMR (JPL)
  - ITRF14 orbit solutions (GSFC and CNES)
  - GDR-F geophysical models (CNES)
- Ongoing work processing Poseidon 1 waveforms (Bignalet-Cazalet, OSTST 2020) using:
  - Onboard SMLE3 before 1995 (waveforms unavailable)
  - Ground retracking after 1995 (Thibaut, 2017)
  - POE-F orbit solution (CNES)
  - GDR-F geophysical models (CNES)
- Product release for TOPEX and Poseidon is expected early 2021
- Acknowledgements: CNES/CLS for the geophysical models, CNES/CLS Cal/Val team, CU and UNH SSB teams, CNES and GSFC POD teams.